

THESIS

COUPLED CONTINUUM PIPE-FLOW MODELING OF KARST GROUNDWATER FLOW IN
THE MADISON LIMESTONE AQUIFER, SOUTH DAKOTA

Submitted by

Stephen Paul Saller

Department of Geosciences

In partial fulfillment of the requirements

For the Degree of Master of Science

Colorado State University

Fort Collins, Colorado

Spring 2013

Master's Committee:

Advisor: Michael Ronayne

Thomas Sale
Sven Egenhoff

ABSTRACT

COUPLED CONTINUUM PIPE-FLOW MODELING OF KARST GROUNDWATER FLOW IN THE MADISON LIMESTONE AQUIFER, SOUTH DAKOTA

Karst carbonate aquifers are traditionally difficult to model due to extreme permeability heterogeneities and non-Darcian flow. New modeling techniques and test applications are needed to improve simulation capabilities for these complex groundwater systems. This study evaluates the coupled continuum pipe-flow framework for modeling groundwater flow in the Madison aquifer near Rapid City, South Dakota. The Madison carbonate formation is an important source of groundwater underlying Rapid City. An existing equivalent porous medium (EPM) groundwater model of the Madison aquifer was modified to include pipe networks representing conduits. In the EPM model, karstified portions of the aquifer are modeled using high hydraulic conductivity zones. This study hypothesized that the inclusion of conduits would allow for a simpler hydraulic conductivity distribution and would improve modeled fits to available data from a 10-year monitoring period. Conduit networks were iteratively fit into the model based upon available environmental and dye tracer test data that approximated major karst pathways. Transient simulation results were evaluated using observation well hydraulic heads and estimated springflow data. In a comparison to the EPM model, the new modeling results show an improved fit to the majority of observation well targets, and negligible impact to springflow data. The flow dynamics of the aquifer model were significantly altered, with the conduit networks acting as gaining or losing subsurface features, behaving as regional sinks during dry periods and flowpath heterogeneities during wet periods. The results of this study demonstrate that the coupled continuum pipe-flow modeling method is viable for use within large regional aquifer models.

ACKNOWLEDGEMENTS

I would like to thank Dr. Andrew Long of the United States Geological Survey for his generous cooperation and assistance with this thesis, as well as the USGS's Larry Putnam for his work on the base model used herein.

I am grateful to Dr. Tom Sale and Dr. Sven Egenhoff for being a part of my committee and offering their valuable time to review this work.

I would like to thank my family and friends for their constant support and good sense of humor.

Finally, I would like to thank Dr. Michael Ronayne, whose guidance, patience, and knowledge were invaluable to the completion of this thesis.

Part of this research was funded by a seed grant from the University Consortium for Field-Focused Groundwater Contamination Research. Their support is gratefully acknowledged.

TABLE OF CONTENTS

ABSTRACT.....	ii
CHAPTER 1 - INTRODUCTION	1
1.1 Research Objectives	2
CHAPTER 2 – REVIEW OF KARST GROUNDWATER MODELING METHODS	4
2.1 Probabilistic Approaches	4
2.2 Equivalent Porous Medium (EPM)	4
2.3 Discrete Fracture Network	5
2.4 Coupled Continuum Pipe-Flow	6
CHAPTER 3 – STUDY AREA DESCRIPTION	9
3.1 Geologic Setting	10
3.2 Site Hydrogeology	13
3.3 Karst Conduit Data	15
CHAPTER 4 – METHODOLOGY	16
4.1 Model Description and Initial Parameters.....	16
4.1.1 Basic Model Information.....	16
4.1.2 Hydraulic Conductivity Zonation	20
4.1.3 Recharge	22
4.1.4 Temporal discretization	23
4.2 Conduit Integration using MODFLOW-CFP	23
4.2.1 MODFLOW-CFP governing flow equations	24
4.2.2 Inferred Conduit Locations	26
4.2.3 Method to locate conduits and assign parameters.....	26
4.3 Spring Discharge Methods	28
4.3.1 Internal approach	29
4.3.2 Coupled Drain approach	30
CHAPTER 5 – RESULTS AND DISCUSSION	31
5.1 CFP Karst Model Information.....	32
5.1.1 Simplification of Hydraulic Conductivity Zones	32
5.1.2 Conduit Geometry	34
5.1.3 Conduit Parameters	37
5.2 Steady State Model	39

5.3 Transient Model Target Data Comparisons	41
5.3.1 Comparison to Measured Hydraulic Heads at Observation Wells.....	41
5.3.2 Comparison to Estimated Spring Flow	47
5.4 Analysis of the Simulated Conduit-Matrix Exchange	51
5.4.1 Conduit-Matrix Exchange Profiles	51
5.4.2 Temporal Variability in Simulated Conduit-Matrix Exchange	54
CHAPTER 6 – CONCLUSIONS.....	57
6.1 Study Summary	57
6.2 Proposed Future Work.....	58
REFERENCES	61

LIST OF TABLES

Table 5.1 Conduit Parameter Values	39
------------------------------------------	----

LIST OF FIGURES

Figure 2.1 Hydraulic head contours depicting a gaining conduit system	7
Figure 2.2 MODFLOW-CFP cell diagram demonstrating possible network connections.....	8
Figure 3.1 Outcrop of the Madison limestone showing karst features.....	9
Figure 3.2 Study area base map	10
Figure 3.3 Geologic Map of the Black Hills region near Rapid City.....	11
Figure 3.4 Hydrogeologic Conceptual Model.....	13
Figure 4.1 Model extent and finite-difference grid.....	17
Figure 4.2 Spring Locations in model layer 3	19
Figure 4.3 Original Layer 3 Hydraulic Conductivity Zones	22
Figure 5.1 Matrix hydraulic conductivity distribution in model layer 3.....	33
Figure 5.2 Conduit Locations	36
Figure 5.3 Steady State Potentiometric Surface for Model Layer 3	40
Figure 5.4 Observation Well Locations Map.....	43
Figure 5.5 Observation Well Comparisons (part A)	44
Figure 5.5 Observation Well Comparisons (part B)	46
Figure 5.6 Model Comparisons to Estimated Spring Flow	50
Figure 5.7 Simulated conduit-matrix exchange flow along Jackson-Cleghorn conduit network..	53
Figure 5.8 Simulated conduit-matrix exchange flow along South Network Conduit Network.....	54
Figure 5.9 Simulated hydraulic heads in the vicinity of Jackson-Cleghorn conduit.	56

CHAPTER 1 - INTRODUCTION

Karst aquifers support the way of life of many communities throughout the globe as an important source of water. As much as a quarter of the world, and an eighth of the United States, rely on karst groundwater systems for all or part of their water supply [Darnault, 2008; Covington et al., 2011]. Growing awareness of the value of understanding and protecting groundwater resources, coupled with rapid advancements in measurement and modeling technology, has brought new interest to these unique aquifers [Covington et al., 2011].

Karst is a broad term for a formation of carbonate rock that has been preferentially dissolved into interconnected voids ranging from small channels to massive caverns [Ford and Williams, 2007]. The secondary porosity in this limestone or dolostone forms at a point in its life cycle when it is near the land surface, where acidic meteoric water can infiltrate and break down the calcium carbonate bonds. As a karst formation matures, the flow pattern transitions from being controlled by many small channels to a subset of those small channels growing and becoming large groundwater conduits. Mature karst systems are responsible for many of the large caves and caverns seen around the globe. These networks will weather in a path of least resistance; smaller conduits will act as branching tributaries that feed into larger conduits in a pseudo-watershed aquifer system [Worthington and Ford, 2009].

The groundwater flow dynamics of these aquifers are still difficult to understand and model, relative to other aquifer types. Karst systems possess both Darcian flow in the matrix and potentially turbulent pipe flow in the conduit openings, which themselves are difficult to track due to high levels of uncertainty in site-specific information [Quinn et al., 2006]. Mathematically, it is a challenge to account for the multiple orders of magnitude difference in velocities between the

open chamber networks and low-permeability matrix zones. Recent modeling developments have begun to address this challenge, as will be discussed in Chapter 2 of this thesis.

In order to improve predictive accuracy, karst aquifer models need to account for the high degree of heterogeneity inherent in these subsurface systems. In addition to a well-defined geologic framework, modeling efforts may require detailed water level measurements, spring gauge data, and an analysis of the connectivity of the aquifer through tracer tests [Darnault, 2008; Scanlon et al., 2003]. Karst aquifer systems are more likely to produce rapid, catastrophic consequences to a contamination event, due to the extremely high groundwater velocities within conduits. These velocities limit the applicability of traditional Darcian-continuum models in karst [Green et al., 2006]. Thus the development of new modeling techniques, informed by hydrogeologic data, is essential.

1.1 Research Objectives

This research project evaluates the coupled continuum pipe-flow modeling framework for simulating complex karst groundwater flow within a large-scale regional aquifer model, with the hope that these systems can become modeled more accurately in the future. An existing equivalent porous medium (EPM) model for the Madison limestone aquifer in South Dakota is modified to include karst conduit flow. The specific objectives of this thesis are as follows. The first objective is to demonstrate that the coupled continuum pipe-flow simulation method can operate effectively at a scale previously unseen. The second is to determine whether an EPM model can be simplified through the introduction of this methodology, while altering as few model parameters as possible. The third objective is to measure how effectively the new model can match observation well hydraulic heads and springflow data. Finally, this thesis will consider

limitations of the coupled continuum pipe-flow framework as currently implemented in MODFLOW and identify areas for future research.

CHAPTER 2 – REVIEW OF KARST GROUNDWATER MODELING METHODS

The unique challenges presented in attempting to model a karst aquifer system have bred a number of unique solutions to accompany them. This large variety of approaches to karst modeling reveals that none have been able to become a true standard. The general approaches tend to fall into four categories: probabilistic, equivalent porous medium (EPM), discrete fracture network, and coupled continuum pipe-flow models. The verbiage associated with karst model terminology is immense and at times contradictory, so when possible alternate terms for a given modeling methodology will be noted.

2.1 Probabilistic Approaches

Probabilistic approaches to modeling karst aquifers are fairly common, as they do not require the wide range of input data that a deterministic parameter-based approach requires. Rather, a statistical analysis of previous system input (recharge) and output (spring flow) is used to predict future system responses by generating spring discharge hydrographs. For the purposes of understanding groundwater movement in the aquifer, this approach is not applicable [Darnault, 2008].

2.2 Equivalent Porous Medium (EPM)

Making use of only Darcian flow, examples within this category include lumped parameter systems, distributed parameter, and single continuum smeared conduit systems [Scanlon et al. 2003]. These models assume that the entire aquifer, including conduit zones, can be treated as an EPM. Generally this involves using the differences between hydraulic conductivity zones in order to obtain the same output features as a karst network. This has been

done many ways, from the Edwards Aquifer lumped parameter mixed zone scheme [Scanlon et al., 2003] to a channel simulation involving high conductivity flowpaths [Worthington, 2009].

These high conductivity models use heterogeneous conductivity zones to simulate a “smeared conduit” effect meant to represent multiple karst conduits running through an aquifer. Through optimization programs, a best fit for a particular steady state output can be built into these systems. When transitioning to recharge event driven transient flow, these fits tend to break down due to water velocity differences [Worthington, 2009; Green et al., 2006; Quinn et al., 2006].

Some investigators have developed EPM models where the conduits are treated as internal sinks. For example, Quinn et al. [2006] developed a MODFLOW model to simulate groundwater flow within the Malm Formation in Germany. In their model, the conduits were represented using long strings of drain cells. Each drain cell has its drainage rate regulated through its conductance term and set elevation, with the drain elevations decreasing as the channels move downstream. This model was able to create an optimized head surface relative to the target observation wells, and could track groundwater movement through the system until hitting the drain cells. The drawbacks of this approach include not simulating the flow once the conduits were reached, and the inability to transition this model to transient flow.

2.3 Discrete Fracture Network

These models only simulate groundwater movement through conduits, with no parameters established for the rock matrix. An advantage of discrete network models that is not represented in EPM models is the ability to simulate turbulent flow. In karst applications, this modeling technique has primarily been used to predict discharge from the conduit network [Darnault, 2008].

2.4 Coupled Continuum Pipe-Flow

This method involves the simulation of both a matrix aquifer and a separate, overlapping conduit system. These two continuums exchange groundwater at their represented contact points in the matrix aquifer, controlled by head differences and an exchange coefficient. In terms of building a system that accurately conveys the physical processes of a karst aquifer, coupled continuum pipe-flow models have the advantage over others in being able to simulate both turbulent conduit flow and laminar matrix flow [Liedl et al., 2003].

The Carbonate Aquifer Void Evolution (CAVE) model is a well-established coupled continuum pipe-flow model for simulating groundwater flow in karst aquifers. Researchers working at multiple sites in Europe have used CAVE to develop steady-state models that consider both matrix and conduit flow, with improved accuracy over the previous standing models [Bauer et al., 2003]. Flow in the conduits is modeled using pipe flow equations that require the input of conduit diameter, roughness, tortuosity, and critical Reynolds number (to determine the onset of turbulence). As noted by Teutsch et al. [1993], the most sensitive parameter within these simulations is the conduit wall hydraulic conductance, which is described in more detail in Chapter 4. Developed as a lumped parameter, it is intended to represent the level of connectivity of the conduit system to the matrix, be it controlled by skin effects dampening the connectivity or micro conduits improving it.

Using the numerical approach implemented in CAVE, Shoemaker et al. [2008] created a conduit flow package (CFP) for MODFLOW. To this point, the MODFLOW-CFP software has primarily been used for either flow between 2 points with constant head boundaries, or flow to a single point with a drain or constant head boundary like in figure 2.1. Prior applications have all been relatively small in scale, single layered, and primarily for evaluation [Shoemaker et al., 2008; Reimann and Hill, 2009; Hill et al., 2010; Gallegos, 2011]. Like CAVE, MODFLOW-CFP

consists of a setting up a conduit pipe network within the larger finite-difference cells used to represent the matrix. As seen in figure 2.2, each node in the pipe network can be connected to a maximum of 6 other nodes. Pipes can gain or lose water to the matrix depending on the hydraulic head gradient. MODFLOW-CFP is the software used in this study to investigate groundwater flow in the karst Madison aquifer.

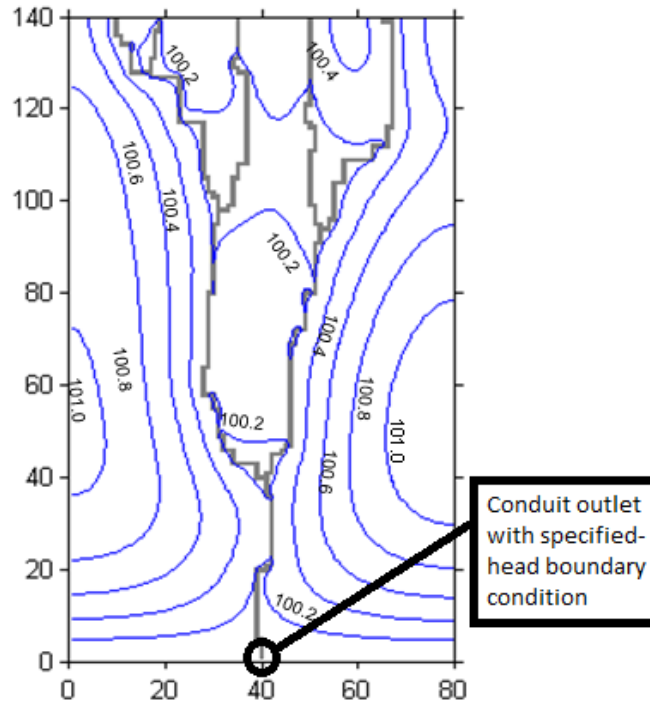


Figure 2.1 Hydraulic head contours depicting a gaining conduit system, simulated using MODFLOW-CFP [from Saller and Ronayne, 2011]

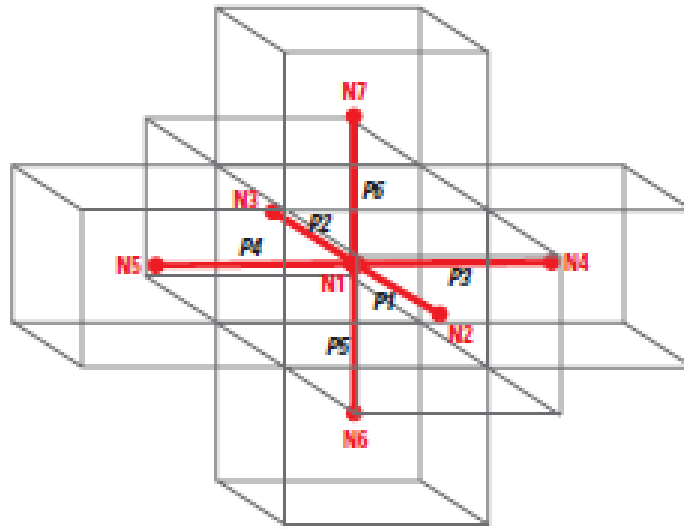


Figure 2.2 MODFLOW-CPF cell diagram demonstrating possible network connections [from Shoemaker et al., 2008]

CHAPTER 3 – STUDY AREA DESCRIPTION

This study considers groundwater flow within a karst limestone aquifer in the vicinity of Rapid City, South Dakota. Rapid City is located just east of the Black Hills, a national forest located on mountainous terrain in western South Dakota. The area is underlain by two limestone formations from which Rapid City draws more than half of its water – the Madison and the Minnelusa aquifers. The Madison in particular is known to be karstified (Figure 3.1), and its springs feed the creeks and rivers that give Rapid City its name.

The numerical modeling presented in this thesis utilizes data collected by the United States Geological Survey (USGS) during a ten year period between October 1987 and September 1997. The aquifer analysis area, seen below in figure 3.2, is roughly 629 square miles and runs from north of Elk Creek to south of Spring Creek, and from the start of the Madison outcrop zone three miles west of Rapid City to seven miles east of Rapid City. There is over 4 thousand feet of elevation difference between the highest points in the western portion of the study area and the lowest of the east.



Figure 3.1 Outcrop of the Madison limestone showing karst features

3.1 Geologic Setting

The geology of the region is the result of a Cretaceous period uplifting event that was then eroded down to form a dome-like structure. West of the study area, exposed Precambrian igneous rock make up the center of the Black Hills dome, shown below in figure 3.3. The geologic formations considered in this study are all Paleozoic in age, and are part of an uplifted ring dipping to the east.

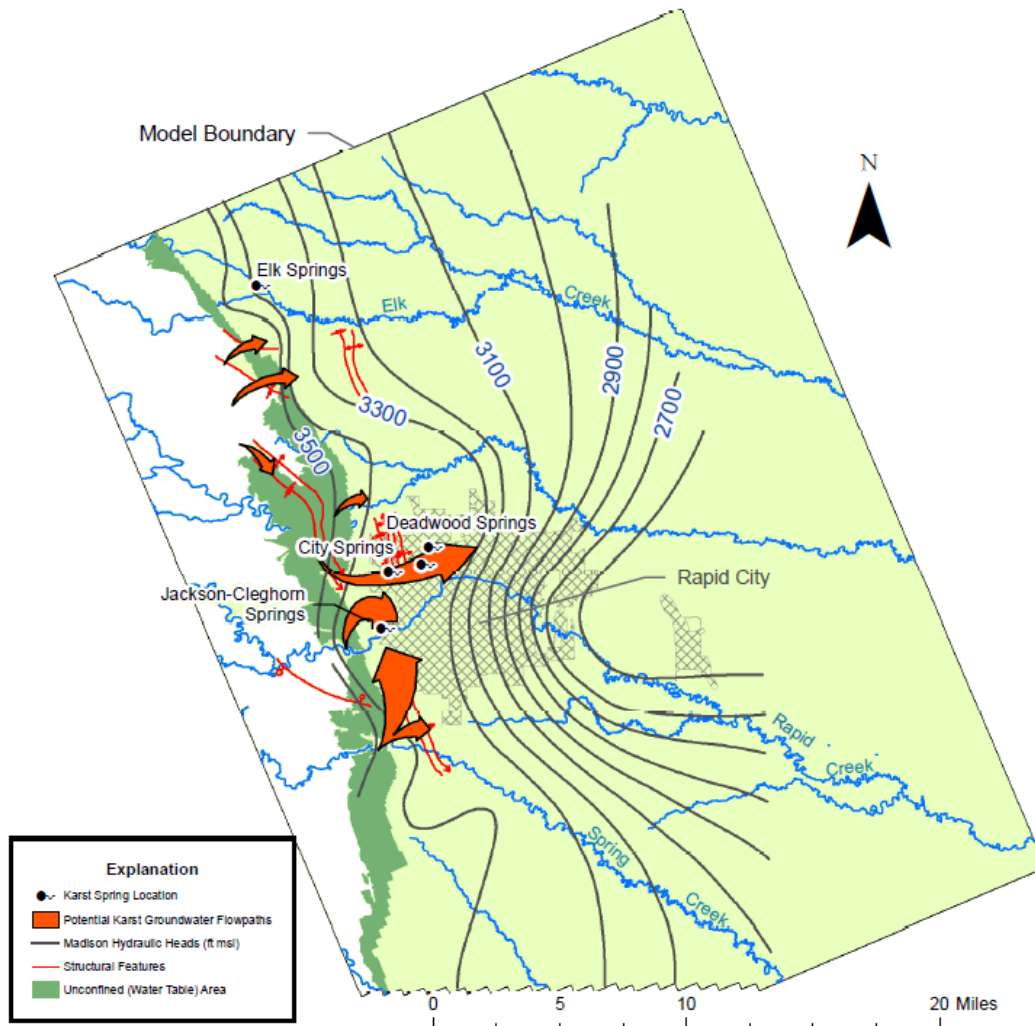


Figure 3.2 Study area base map

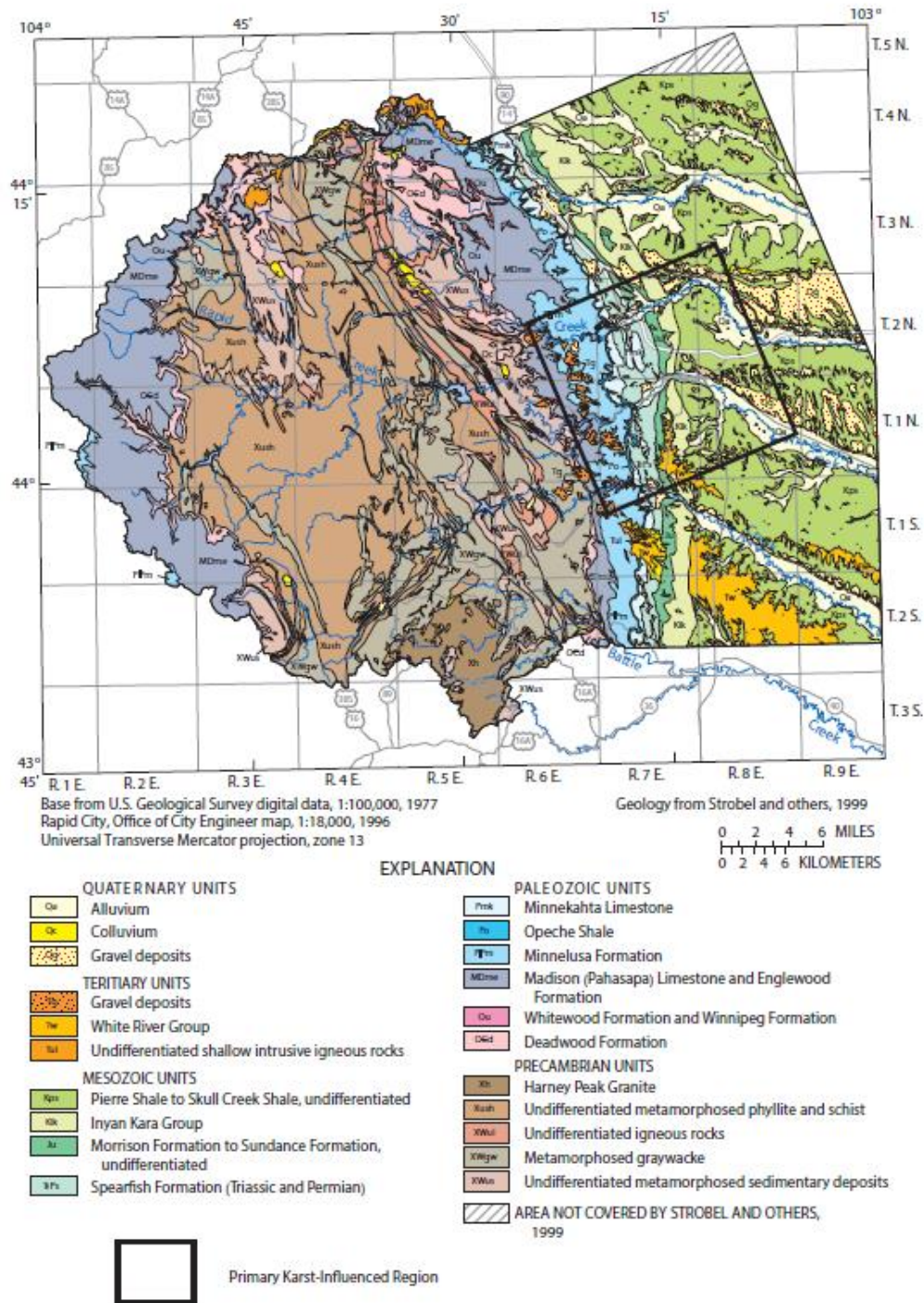


Figure 3.3 Geologic Map of the Black Hills region near Rapid City [modified from Long and Putnam 2002]

The Madison Limestone is Mississippian in age, and ranges from 250 to 550 feet thick [Long and Putnam, 2002]. It is a massively bedded limestone, primarily light in color, partially dolomitized, and karstified in the upper 100 to 200 feet of the formation. The lower portion of the formation is thought to be much less permeable [Greene, 1993]. The Englewood formation, a thin Devonian aged limestone ranging from 30 to 60 feet thick, is directly below the Madison formation and for the purposes of this study is lumped together with the less permeable lower portion of the Madison limestone.

The Minnelusa Formation was deposited in both the Pennsylvanian and the Permian, and ranges from 375 to 800 feet thick. It consists of cross-bedded and interbedded limestone, sandstone, dolomite, shale, and anhydrite. The upper 200 to 300 feet of the formation is considered the high permeability zone, consisting of coarser grains and collapse features [Bowles and Braddock, 1963]. The lower portion is primarily discontinuous shale with some interbedded limestone and sandstone, and is considered the low permeability zone of the formation.

The Ordovician aged Whitewood and Winnipeg Formations and the Cambrian aged Deadwood Formation are lumped as one 75 to 560 foot hydrogeologic unit, and as a group referred to as the Deadwood Formation [Long and Putnam, 2002]. The Whitewood consists of dolomite and limestone, the Winnipeg is comprised of shale and siltstone, and the Deadwood is a mix of sandstone, shale, dolomite, and limestone conglomerates. These formations outcrop to the west of the Madison and Minnelusa outcrops, and are the last sedimentary rock units before hitting igneous and metamorphic bedrock [Cattermole, 1969].

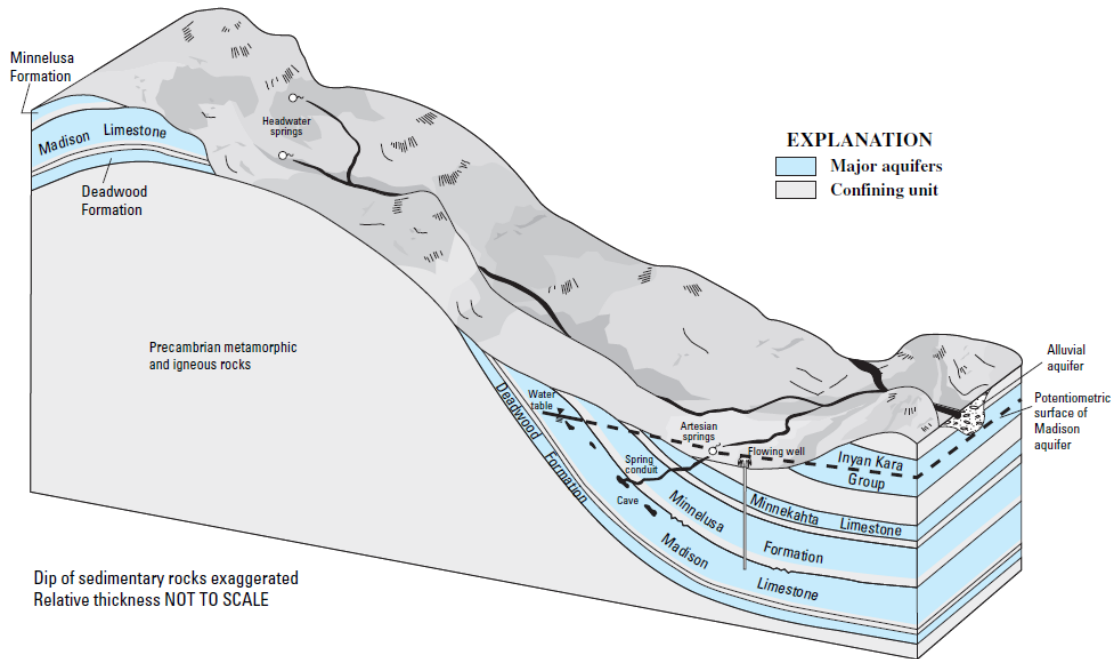


Figure 3.4 Hydrogeologic Conceptual Model [from Putnam and Long, 2007]

3.2 Site Hydrogeology

The hydrogeologic features of the aquifers beneath the Rapid City area are well documented, with years of pump test, groundwater level, and spring gauge data collected by the USGS. For this study, the hydrogeologic conceptual model developed by Long and Putnam (2002) was adopted. This conceptualization recognizes three primary aquifer units: the Minnelusa, Madison, and Deadwood aquifers. The aquifers dip to the east and are known to be under confined, artesian conditions (Figure 3.4). Faults, breccia pipes, and chemical weathering (karst) features link to springs on the surface in several known locations within the study area. The modeling research presented in this thesis focuses on groundwater flow within the Madison limestone, which is the aquifer unit that has undergone the most karstification.

Transmissivities estimated from pump tests in the Madison aquifer range from 500 to 20,000 ft²/d [Long and Putnam, 2002]. This wide range is due to a high degree of anisotropy and heterogeneity throughout the region, as well as the presence of karst conduits that strongly influence pump-test response data. The potentiometric surface of the Madison aquifer contains numerous shifts in gradient magnitude and direction (Figure 3.2). This can be attributed to a high degree of heterogeneity due to karst and other permeability manipulating features.

Water is supplied to the Madison and Minnelusa aquifers from three primary sources. Meteoric water is introduced into the Madison and Minnelusa aquifers from precipitation seeping into the exposed outcrop rock in the western portion of the study area. Additional water moves into the aquifers from several losing streams along the outcrops, which will be referred to as streamflow recharge in this study. The final source of inflow is groundwater influx from the Deadwood aquifer that underlies the Madison; it possesses an up flowing gradient and supplies a small amount of recharge [Long and Putnam, 2002].

Water is discharged from the Madison and Minnelusa aquifers by natural mechanisms and by anthropogenic groundwater pumping. Artesian springs are found in each aquifer, though there is much more spring flow from the Madison aquifer due to higher hydraulic heads in this unit. Pumping wells are active in each aquifer, with some municipal wells pumping at high rates (> 360,000 ft³/d). These wells are found throughout the study area, but are primarily located around the Rapid City region. Groundwater also exits the study area along the eastern border along the general gradient flow path (Figure 3.2).

3.3 Karst Conduit Data

Karst pathways and conduit information for the Rapid City area has been collected through a number of dye and environmental tracer tests. Two primary dye tracer tests have been used to categorize karst conduit areas in the region. In 1993, a dye tracer test was performed into the Boxelder Creek loss zone. This dye was detected at 4 observation wells and at City Springs, and indicated a general flow pattern for the karst aquifer [Greene, 1999]. Putnam and Long [2007] later performed a fluorescein dye test that delineated a conduit network starting at the Spring Creek loss zone and moving in the direction of Jackson-Cleghorn Springs.

Environmental tracers including oxygen isotopes, chlorofluorocarbons, electrical conductivity, and tritium were measured in 1999, 2001, and 2005 at multiple well sites around the Rapid City region [Strobel et al., 1999; Naus et al., 2001; Long et al., 2008]. Zones with a higher level of water velocity and interaction can be estimated from zones of lower average water age and similar groundwater properties. As seen in figure 3.2, these zones tend to propagate either in line with or perpendicular to the predominant faulting patterns through the region. The flow patterns observed in the dye tracer studies generally coincide with the environmental tracer contours.

CHAPTER 4 – METHODOLOGY

Putnam and Long (2009) developed an equivalent porous medium (EPM) model for the Madison and Minnelusa aquifers in the study area. This existing groundwater flow model was utilized as the base case for this study. The scale, scope, and complexity of the model makes it an excellent proving ground to test the coupled continuum pipe-flow capabilities in MODFLOW-CFP. Section 4.1 below provides an overview of the model and describes the initial EPM parameterization that was used by Putnam and Long (2009). The coupled continuum pipe-flow framework and site-specific implementation of this method is discussed in Section 4.2. Section 4.3 describes the technique that was used to simulate spring discharge in the new model that includes conduits.

4.1 Model Description and Initial Parameters

4.1.1 Basic Model Information

The Putnam and Long (2009) numerical groundwater model of the Minnelusa and Madison hydrogeologic units was developed using two different programs: MODFLOW [Harbaugh et al., 2005] and PEST [Doherty, 2002]. In this study, the MODFLOW version will be reviewed and expanded upon exclusively. The model was put together using the MODFLOW-2000 edition.

The MODFLOW model represents a total area of approximately 993 square miles, contains 5 layers, and is split into 105,501 active cells that are divided by a grid of 221 rows and 169 columns (Figure 4.1). These cells are split into different spacing zones, with denser spacing

toward the primary study area to the west of Rapid City. At their most dense, these cells are 492 x 492 foot squares. At their most spacious, the cells are 1640 x 6562 foot rectangles. These larger cells are the furthest away from the primary study area, to the east of the city. Layers 1-4 are similar in general layout, with each successive layer moving the no-flow barrier that represents the formation's western outcrop further to the west. Layer 5 is almost entirely inactive no-flow cells, with a narrow region that represents the Deadwood formation's outcrop and area to interact with layer 4.

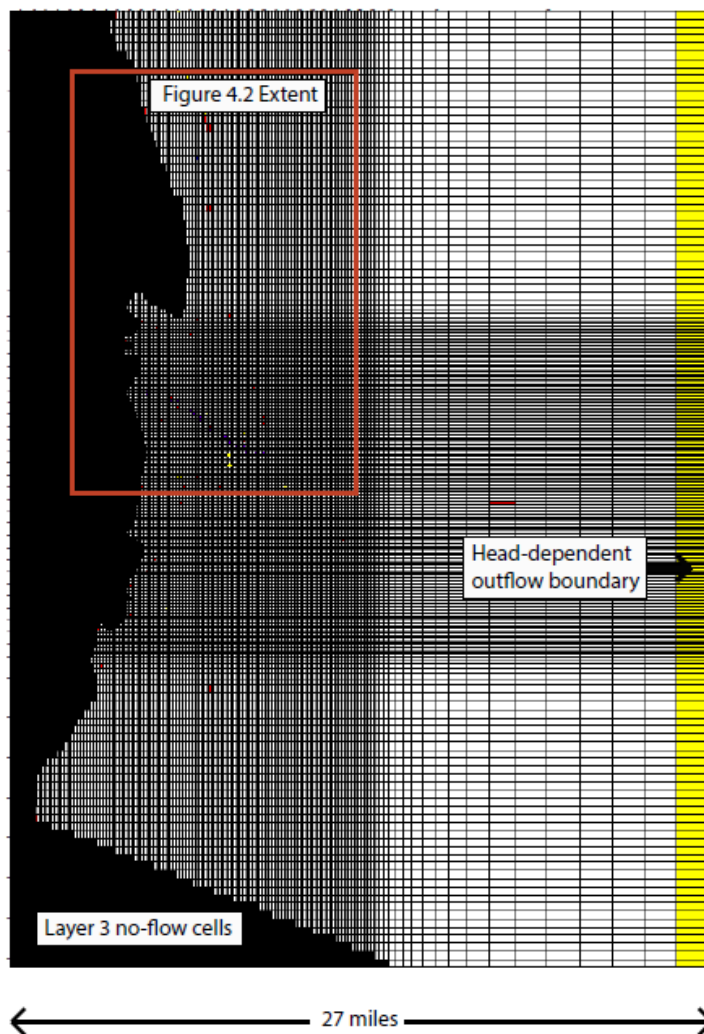


Figure 4.1 Model extent and finite-difference grid

There are 905 drain cells, 141 well cells, 11 river cells, 332 cells lined with a horizontal flow barrier that represents a fault structure, and 81,244 inactive no-flow cells contained in the model. The model is bounded by impermeable boundaries to the west, north and south, and a wall of drain cells (head-dependent boundary) to the east in all but layer 5, which is bounded by no-flow cells. The north and south edges serve as flow line boundaries (i.e., regional groundwater flow is parallel to these boundaries). There are additional drains in the model apart from the eastern model border, each of which represents an artesian spring from the permeable section of either the Minnelusa or the Madison. These can be split into seven primary spring systems: Jackson-Cleghorn Springs, City Springs, Deadwood Springs, Elk Springs, Boxelder Springs, Infiltration Gallery Springs, and Canyon Lake. Each spring system can represent multiple drain cells on either layer 1, 3, or both. The hydraulic conductance for each drain cell was adjusted to optimally fit the available spring discharge data collected by stream gauges and estimates. The largest discharge values come from the Jackson-Cleghorn Springs system; with a simulated average discharge of 20 cubic feet per second, Jackson-Cleghorn Spring accounts for roughly 63% of the total spring discharge for the model. The locations of each of these drain-represented spring systems are shown in figure 4.2.

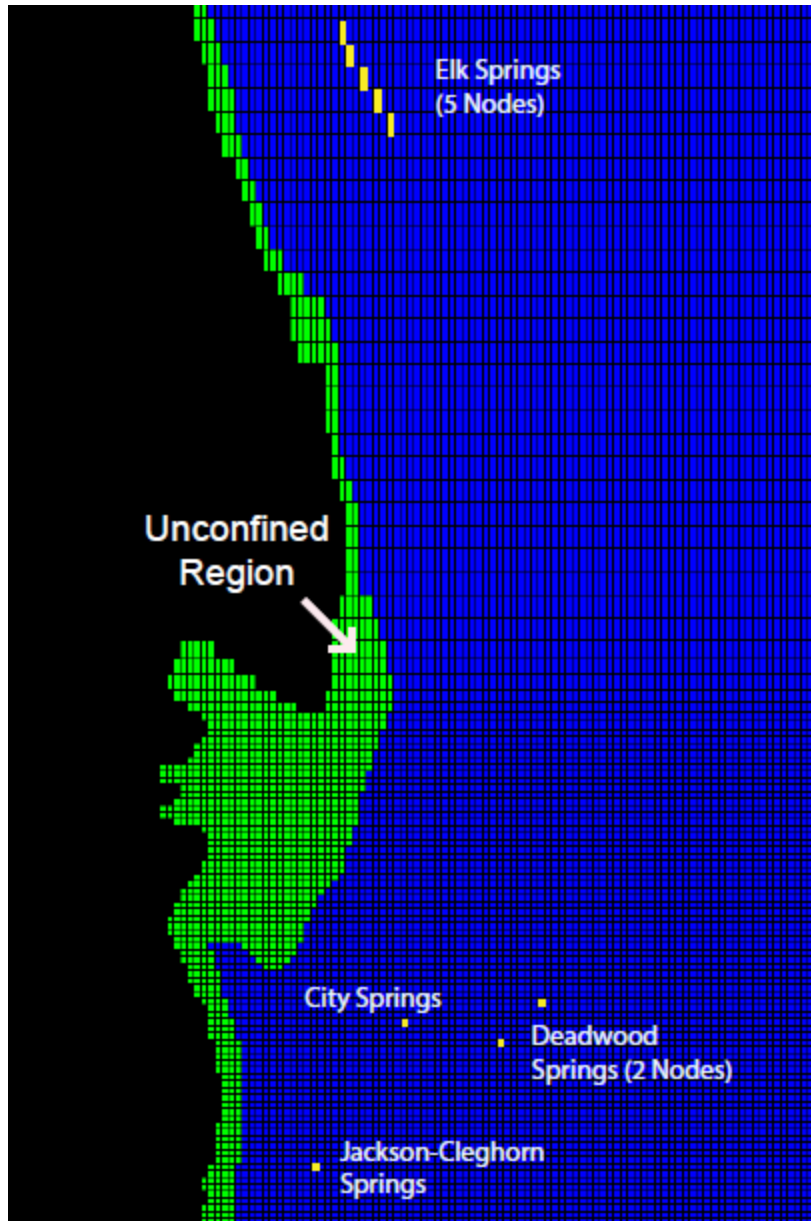


Figure 4.2 Spring Locations in model layer 3

Well cells are divided into 2 primary types – pumping wells that represent municipal water wells, and injection wells that represent sinkhole zones that supply deep aquifers. The pumping wells are scattered across the model, but are mostly found in the Rapid City area. The injection wells, geologically classified as either large karst sinkholes or breccia pipe sinkholes,

are mostly found along the western model edge of layers 1 and 3. Detailed bi-yearly average pumping values are recorded and used for each extraction well – in many cases, the pumping only occurs in relatively few of the model stress periods. These cells, along with the river cells in layer 1, the Horizontal Flow Barrier (HFB) cells in layers 1-4, and the no-flow cells, have not been altered from their original locations and specifications in the EPM model.

The numerically modeled Minnelusa and Madison aquifers are set as confined in MODFLOW, but a brief unconfined section is simulated in each layer by altering specific storage values. The bulk of each modeled aquifer model falls under one primary lower storage zone, however, there additional storativity zones found in the model in each layer. One lines the western portion of each aquifer as the general western outcrop region. Another storage zone, this one found only in layer 3, covers an anticline area where the Madison outcrops again. These additional zones represent areas interact with the areal and streamflow recharge of the system, simulating a partially unconfined section that will store a portion of the recharge water and delay its movement to the rest of the model.

4.1.2 Hydraulic Conductivity Zonation

Horizontal hydraulic conductivity is the primary driver of the simulated groundwater gradients in the model. In the Putnam and Long (2009) model, this important parameter has been divided into multiple separate zones per layer, the magnitudes of which were estimated using field data and model calibration. Layer 1, the permeable upper Minnelusa formation, is divided into 3 hydraulic conductivity zones, with values ranging from 0.1 to 388.8 feet per day. Layer 2, the less permeable lower Minnelusa, is set up into similar zones, but each horizontal conductivity value is set to one-tenth of its counterpart in layer 1.

Layer 3 represents the upper permeable portion of the Madison limestone and is the focus of this study. The initial parameterization of layer 3 included seven different horizontal

hydraulic conductivity zones – HK3_1 through HK3_7 (Figure 4.3). Conductivity zones HK3_4, 6, and 7 are thought to contain karst features, as observed in dye tracer tests at Boxelder and Spring creeks. Consequently, these zones were assigned higher effective hydraulic conductivity values. Zone HK3_6 in particular was assigned a high value of 389 feet per day, which allows for high simulated discharge at Jackson-Cleghorn Spring. Conductivity zones HK3_2, 3, and 5 are assigned relatively lower conductivity values to represent less karstified areas in the Madison aquifer. Zone HK3_1 was assigned a relatively high conductivity value based on field measurements reported by Downey (1986), but this zone is toward the eastern portion of the model, away from the karst springs, and therefore is not considered in this study. Similar to layer 2, layer 4 matches the horizontal conductivity values of layer 3, but each is one-tenth of the layer 3 value. Layer 5, representing the Deadwood aquifer, is assigned a single low horizontal conductivity value.

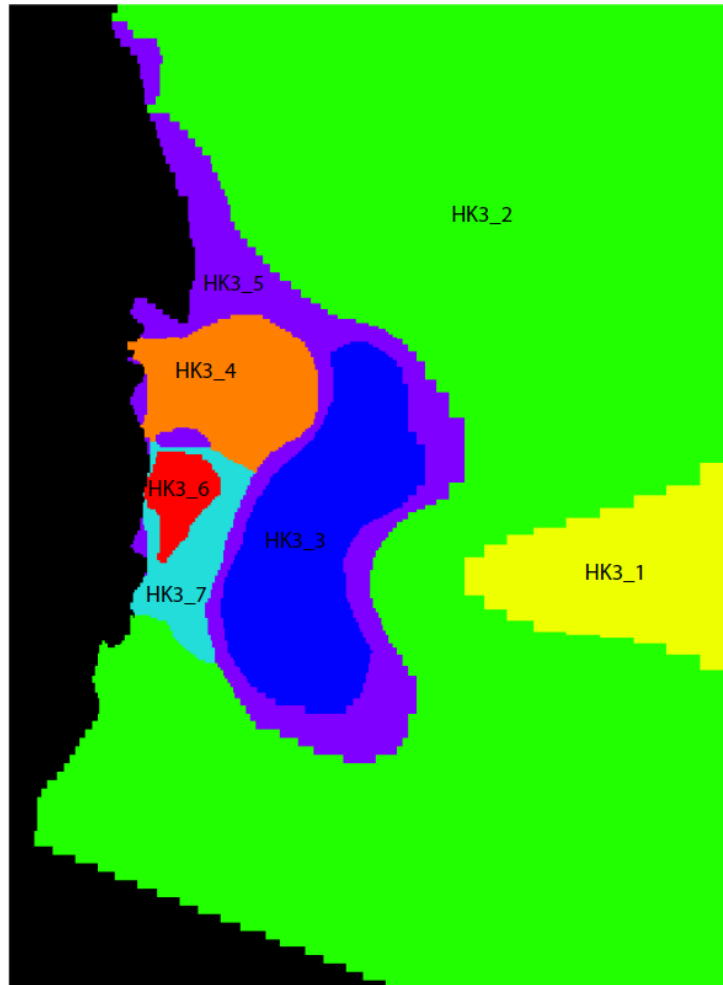


Figure 4.3 Original Layer 3 Hydraulic Conductivity Zones

4.1.3 Recharge

Areal recharge is introduced to each model layer in the westernmost cells, which represent each formation's surface outcrop. The recharge data was estimated for each model stress period using available precipitation data minus calculated evapotranspiration and surface water catchment. This data was split into 5 zones shown below in figure 4.3. This consistent water supply from the west being driven to the drain cells that form the eastern border helps create the general eastern gradient that dominates the model. The highest recharge zone is

zone 2, which represents from Little Elk creek to Boxelder creek. The lowest is zone 4, from Rapid Creek to Spring Creek.

Streamflow Recharge is a large component of water mass inflow into the system – with a higher total input value than areal recharge. For the Madison aquifer in particular, streamflow recharge accounts for roughly triple the total input of areal recharge in the dry period, and roughly double in the wet period. Intended to represent sinkholes and known disappearing streams, a select number of cells represented with injection wells have been assigned an estimated total inflow number derived from runoff and stream flow estimates [Long and Putnam, 2002; Putnam and Long, 2009].

4.1.4 Temporal discretization

The model is transient and is based on data collected over a ten year period from 1987-1997. This time span is simulated using 20 model stress periods, each representing 6 months. At this temporal scale, effects from individual storm events or short term pumping events will be lost and blended into a longer-term average behavior. The 10-year simulation period includes a dry span of years followed by a relatively wet span of years. The first 11 stress periods (1987-1993) comprise the dry period, and the remaining nine stress periods (1993-1997) represent the wet period.

4.2 Conduit Integration using MODFLOW-CFP

The primary objective of this project was to evaluate the coupled continuum pipe-flow modeling approach for simulating karst groundwater flow in a regional aquifer model. MODFLOW-CFP was used to implement this approach. Introducing conduits was an iterative process that involved placing, defining and optimizing conduit networks based on limited

information. Once the conduit networks were set, changes in model performance could be observed and analyzed. One way to observe those changes is to note differences in model functionality and the regional potentiometric surface maps. Further performance observations can be made by comparing the model results to relevant transient observation data. Achieving an improved fit to the observed springflow and observation well head values over what was previously achieved with an EPM model would suggest that the coupled continuum pipe-flow framework is a promising approach. To directly compare to a heterogeneous EPM model, the new MODFLOW-CFP model merged four hydraulic conductivity zones that were known karst regions and set them at a single lower conductivity value. This allowed for the shape of the groundwater flow through the region to be controlled primarily by the new conduit networks. This study focused on hydraulic conductivity values. Other parameters such as storativity, areal/streamflow recharge distribution, and pumping rates were left unchanged from the EPM model. The only other altered parameter was the drain conductance for karst springs in model layer 3.

4.2.1 MODFLOW-CFP governing flow equations

MODFLOW is a finite-difference groundwater modeling program that computes heads at each cell within the model relative to each adjacent cell, with respect to boundary conditions and system parameters. The Conduit Flow Process package newly introduced to MODFLOW couples this Darcian flow with groundwater movement governed by pipe flow equations in a separate domain that represents the conduits [Shoemaker et al., 2008]. There are 2 primary pipe flow equations this program uses to compute the volumetric flow rate of water moving through each pipe – one for laminar flow (4.1) and one for turbulent flow (4.2), as determined by a computed Reynold's number:

$$Q = -A \frac{\rho g d^2 \Delta h}{32 \mu \Delta l \tau} \quad (4.1)$$

$$Q = -\sqrt{\frac{|\Delta h|gd^5\pi^2}{2\Delta l\tau}} \log\left(\frac{2.51v}{\sqrt{\frac{2|\Delta h|gd^3}{\Delta l\tau}} + \frac{k_c}{3.71d}}\right) \frac{\Delta h}{|\Delta h|} \quad (4.2)$$

For laminar flow, the volumetric flow rate is computed for each pipe tube using Equation 4.1. In this equation, Q [L^3/T] represents the volumetric flow rate of groundwater in the tube, A [L^2] represents the pipe area perpendicular to flow, ρ [M/L^3] is the water density, g [L/T^2] is the gravitational acceleration, d [L] is the pipe diameter, Δh [L] is the change in head over the length of the pipe in that cell, μ [M/LT] is the viscosity of water, Δl [L] is the distance the pipe runs in the cell, and τ is the tortuosity of the pipe [Shoemaker et al., 2008]. The tortuosity is a unitless value that serves as a multiplier to Δl , used to increase the total length of the pipe in the cell to represent bends and twists. From this equation, a velocity followed by a Reynold's number can be computed. If the Reynold's number is above the set turbulent limit, the flow for the cell is found again using the turbulent flow equation instead.

For turbulent flow, the rate is computed using a more complex equation (Equation 4.2) that includes input from all the variables above, but with velocity and pipe roughness variables included. The pipe velocity is represented with the variable v [L/T], and the mean roughness of the pipe wall is represented by the variable k_c [L]. A higher roughness value represents a rough pipe that will lower the volumetric flow rate in turbulent flow, and a lower value represents a smoother pipe that has a negligible impact on this rate [Shoemaker et al., 2008].

The pipe network is connected to the matrix continuum by an exchange equation:

$$Q_{ex} = \alpha_{j,i,k}(h_{in} - h_{j,i,k}) \quad (4.3)$$

The volumetric exchange flow (Q_{ex}) is determined by the difference of the head at conduit pipe node (h_{in}) and the head in matrix cell that node in is within ($h_{j,i,k}$), all multiplied by

the conduit wall conductance ($\alpha_{j,i,k}$) [L^2/T]. This conductance term acts as a flow rate buffer; the lower the value, the less connected the conduit system is to the surrounding rock matrix [Shoemaker et al., 2008]. Conduit wall conductance has been identified as one of the most sensitive parameters in the CFP input system [Reimann and Hill, 2009], and that has held true in this study. Control over flow into and out of the system directly corresponds to volumetric pipe flow rates, discharge flow rates, and matrix flow influence.

4.2.2 Inferred Conduit Locations

The first step in introducing conduits to the model is to understand the general areas karst features should be located in and what directions they should be oriented. As discussed in Section 3.3, multiple tracer studies have revealed the general locations of high conductivity and rapid transport zones within the upper Madison limestone. Though there is no specific karst conduit geometry data, these previous tracer tests provide enough overlapping information to create estimated preferential pathways within the aquifer. Putnam and Long (2002) specifically noted eight potential groundwater flow paths that were thought to be heavily karstified (Figure 3.2). The pathways shown in this figure were used to guide the placements of karst conduit networks within the model.

4.2.3 Method to locate conduits and assign parameters

Once a general orientation was chosen for a conduit network, an iterative process of parameter fitting started. The first step in this process was to construct the geometry of the karst network. Cell by cell, generating a karst network shape without distinct shape involves placing the network in the region assigned to it, and then adjusting it repeatedly until it is moving enough water to satisfy the spring and well conditions down gradient. In this process, ample spacing for conduit branch arms proved important. Too tight a grouping of conduit branches could deplete an upgradient area of water too quickly, resulting in conduit model errors derived

from early backflow. The next phase in setting the geometry was to establish the conduit elevation levels. To keep a standard since this information was unavailable, each node was set 10 feet from the listed top elevation of each layer 3 cell.

Upon the geometry of a conduit network being completed, the next step involves iteratively setting conduit parameters to fit the groundwater movement needs of the model. In this exercise, conduit roughness and tortuosity were left at preset values of 0.001 ft and 1, as were the given upper and lower Reynold's numbers. This left two conduit specific parameters to determine – conduit diameter and conduit wall hydraulic conductivity, which is part of the exchange term that determines the rate of fluid exchange between the matrix and conduit. In general, a larger value of either of these terms leads to greater groundwater flow down gradient. This is not always the case though, as higher exchange in a lower head area will draw out more water from the conduit network. A balancing act is required between conduit geometry, diameter, and exchange flow in order to create a working network. The typical iterative order in fitting these parameters began with setting the conduit geometry, a diameter, an exchange term, then adjusting the exchange term until the model would solve. Once an acceptable exchange term was set, the current value for groundwater transport downgradient was found, then a decision on whether to increase or decrease to flow generated by this conduit network was made. Upon making this decision, the conduit diameter was adjusted, followed by the geometry. The larger a conduit network's diameter was set, the greater the discharge flow up to a certain point, after which the discharge would level off. This limit is the product of the interplay between available cross sectional pipe flow area and increasing surface area for exchange flow; eventually, the higher levels of available exchange flow will result in more flow exiting into the matrix prior to discharging. When this limit is reached, the network geometry needs to be supplemented with either branches or extensions. Once these new parameters are set, the process begins anew and continues until an optimal groundwater movement is found. As more

networks are added, minor parameter adjustments to previously created conduit networks often becomes necessary, especially in cases where these networks are in close proximity to one another. Not every network created for this project ended in a known spring location, but those that did needed a method for simulating that extraction of groundwater from the model.

4.3 Spring Discharge Methods

To simulate the effects of a karst driven spring system, a repeatable and practical method for removing water from set points in the model is necessary. Within MODFLOW, this requires the specification of an internal boundary condition that can act as a local sink. For a confined system like this, the given options were either an extraction well, a constant head location, or a drain cell. Selecting from these options, extraction wells were immediately ruled out, as they require pre-set pumping rates that would not be usable for predictive modeling in future work. Matrix cell constant head boundaries, applied over the entire finite-difference cell, could remove too much water and unrealistically influence the aquifer heads; therefore this approach was also ruled out. MODFLOW-CFP allows for a node to have a constant head boundary within the conduit system. This approach can potentially be implemented without draining the system because the exchange rate between the conduit system and the matrix surrounding this constant head cell would be limited by the network's exchange rate coefficient. As another alternative, drain cells can work as spring discharge points, which is the approach used previously by Putnam and Long [2009] in the EPM model. Both of these latter two methods were evaluated during model development in this study.

4.3.1 Internal approach

There are several benefits in using an internal constant head when using the MODFLOW Conduit Flow Package. The thought of keeping all the karst groundwater movement within the network system until it is discharged is appealing for karst spring simulations. Additionally, the model tends to solve quicker and with less chance for failure using internal constant heads. This is thought to be due to a more defined gradient within the network, and less exchange flow down gradient. When creating a conduit network in this manner, it is important to decrease the conduit wall conductivity on the cell with the internal constant head boundary an appropriate amount, or a sizable percentage of the flow moving to the boundary will be directly from the surrounding matrix.

Though this spring simulation method has several advantages, there is one primary modeling dilemma that an internal constant head boundary can run into: back flow into the system. If the surrounding matrix loses enough water over time to become lower than the set constant head boundary, that boundary will begin to supply the network, and ultimately the surrounding matrix with groundwater. While this makes sense for the applications a constant head boundary is usually intended to simulate, such as a very large lake or ocean, in replicating a spring it is a fatal weakness that negates the boundary condition from acting properly. Through the iterative process of selecting a spring discharge method, certain springs developed this issue during some of the dryer model stress periods. Even though with multiple adjustments these springs eventually were not returning water to the system, this option was abandoned with the thought that in future predictive work, this issue would return when a dry period presented itself again.

4.3.2 Coupled Drain approach

The application of drain cells, which require a pre-set stage elevation and a drain conductance value that controls the rate at which water can leave, is a common way to simulate spring discharge [Quinn et al., 2006; Hill et al., 2010]. The appeal of the using a drain over a constant head system is when the water levels fall below the stage elevation, though no water is discharged from the system, no water flows back into the system either. This benefits the model greatly in matching the hydrogeologic profile of the spring system. In relation to being used in conjunction with CFP, the conduits become a high conductivity pathway to the discharge cell, but there is a disconnect between the water dumped into the cell by the conduits and that water being discharged through the drain system. In general, the concern becomes that the model loses the uniqueness of the spring exit flow being dominated by the conduit system. This issue can be dealt with by adjusting the drain conductance, and to a lesser extent the stage elevation, to greatly reduce the level of drain discharge derived from the surrounding matrix, and increase the role of the conduit driven groundwater in the discharge profile. Additionally, the conduit wall conductivity parameter at the drain cell should be increased to allow for a preferential system exit. In this project, the four spring systems that were modeled with conduits averaged out with between 86 and 100 percent agreement between the amount of groundwater delivered to the drain cells by the conduits and the amount of water discharged by that drain.

CHAPTER 5 – RESULTS AND DISCUSSION

The goal of this conduit flow process integration into the numerical Madison Aquifer model was to bring the model closer to its observed transient target data while simplifying the conductivity zones in the karst occupied model area. In theory, being able to use rapid transport pipes to simulate chemically-weathered karst conduits should match the real world conditions closer than relying exclusively on Darcy's Law. With the information as to the nature of the karst networks limited to general regions and average spring discharge rates, much of the work for this project involved constructing reasonable representations of these networks. In reality, these networks are significantly more complex than the modeled representations used in this study. The nature of chemically weathered limestone suggests that each primary karst conduit is connected to several tributary conduits formed in relation to structural weaknesses due to faulting and preferentially weathered material due to sedimentation patterns. The scale of the numerical model used here, with the smallest cells being nearly 500 x 500 feet, prevents this literal accuracy from being simulated, as only 1 conduit node with up to 6 connecting tubes can occupy a single cell. Rather than attempt to model subgrid-scale details, the goal of these simulated karst conduit networks is to produce a generalized system similar to an EPM "smeared-conduit" network, but with more realistic conduit flow dynamics and matrix exchange behavior. After an iterative process of network geometry and parameter fitting, a final transient model of Minnelusa and Madison aquifers using MODFLOW-CFP was completed.

5.1 CFP Karst Model Information

5.1.1 Simplification of Hydraulic Conductivity Zones

An important hypothesis for this study was that the direct simulation of conduits would allow for a simpler hydraulic conductivity (K) distribution in the matrix. Figure 5.1 compares the horizontal K zonation in the new CFP model to the previous zones used in the EPM model. The inclusion of conduits allowed for two fewer K zones. To accomplish this, the zones that had higher conductivity values representing karst areas (388.7, 39.3, and 22.9 ft/day) were merged and set to 22.9 ft/day, the lowest conductivity value of the group. Though this value is still high for hard rock, it is necessary for the model - not every secondary porosity feature can be simulated using the CFP package. Portions of a low conductivity zone (1.4 ft/day) that were in between the karst regions were also merged into the new area. Seen in figure 5.1, this new zone stretched from the Madison outcrop just above Boxelder Creek to just below Spring Creek. This new singular conductivity zone became the stage for the majority of the karst conduit networks added afterward.

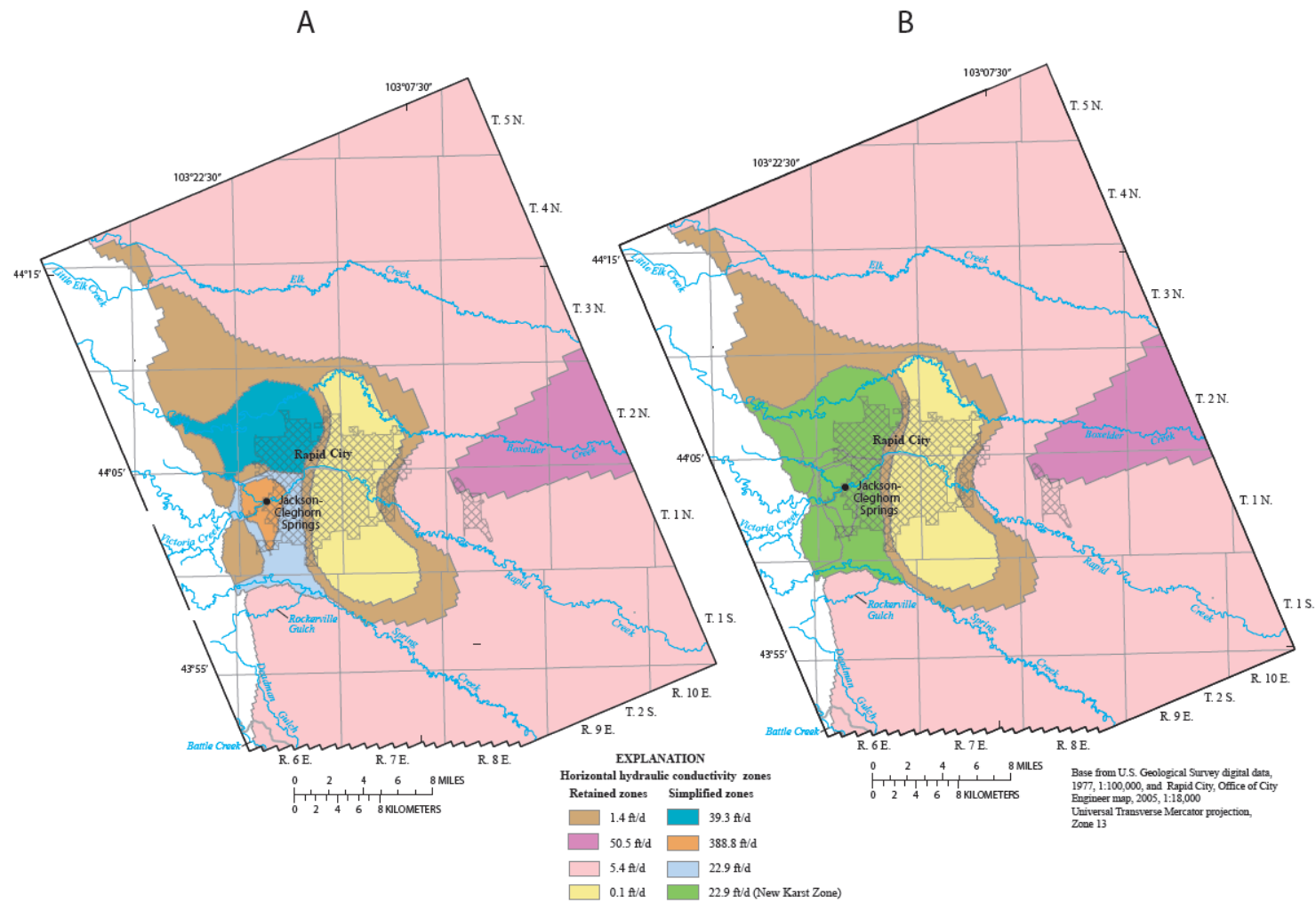


Figure 5.1 Matrix hydraulic conductivity distribution in model layer 3. (A) EPM model. (B) CFP model.

5.1.2 Conduit Geometry

Where to generate the CFP nodes that form the conduit networks within this numerical model entailed a combination of prior tracer data and trial and error. With the only set rule that each modeled spring in layer 3 needed a conduit network, the networks were shaped along highly generalized potential flow paths derived from environmental tracer studies [Section 3.3; Figure 3.2]. The majority of the structural features of the Madison formation are oriented at roughly a 23 degree counter-clockwise strike [Putnam and Long, 2009]. These features include synclines, anticlines, and fault structures. In general, the rock joints which indicate stress weaknesses of the region will align with, and perpendicular to, these features. Karst is formed under preferential chemical weathering of limestone and dolostone rock, and is often oriented corresponding to the formation's structural weakness. This geologic process understanding was another source of information that guided the modeled conduit geometry.

Starting at the southern portion of the model, the orientation of the Jackson-Cleghorn karst conduit network was built along a flow path determined through both dye and environmental tracer studies [Long et al., 2008, Green, 1999; Figure 5.2]. The track also corresponds to the syncline and anticline features directly to its east. The modeled network begins near Spring Creek and migrates north until it hits its discharge location along Rapid Creek. Tributary branches were added to the track to increase its connectivity to the western recharge features, which improve discharge responsiveness and increase conduit flow.

Approximately two miles north of Jackson-Cleghorn Springs is the first of two conduit networks that were built into the model with no spring connected to the model. Instead this network (designated SDET) and its partner act as high conductivity pathways to move water through the now unified matrix conductivity zone. The two are separated by a horizontal flow barrier within the model, which represents a large fault thought to block the majority of

groundwater flow directly south of City Springs. SDET's location is within a possible flow path area marked by environmental tracer tests [Green, 1999; Figure 5.2], and connects a path along a syncline/anticline pair that ends near rapid creek. Two connected branches were added to increase the overall conduit flow.

North of the fault dividing the area there are three distinct conduit networks, two ending in springs, which are all grouped closely together and influence each other greatly. Initially, short conduit networks were generated to feed City Springs and Deadwood Springs, but they were not receiving enough groundwater under the new lower horizontal conductivity of the system to match observed spring discharge rates. A third network, designated NDET, was constructed alongside another syncline/anticline pair to act as a high conductivity pathway and supply the region. NDET begins around Boxelder Creek and ends near City Springs. This network was not directly linked to the other two networks to reduce conduit flow and limit its overall effect on the region. The City Springs conduit network is short and linear, moving directly south of its origin near the endpoint of NDET and down to its discharge point along the horizontal flow barrier. The Deadwood Springs conduit network bifurcates in order to discharge in two separate spring locations; each of the Deadwood Springs locations are thought to be part of the same system and were presented as such in the previous numerical model, so this aspect remains unchanged here.

The conduit network geometry of Elk Springs differs from the other conduit networks with its five discharge cells, each fed by its own conduit tributary split from the primary karst network. The system is at the northern edge of the model (Figure 5.2), linking two possible flow paths from prior environmental tracer studies and running them along the western edge of the model north of a monocline. This orientation is similar to the syncline/anticline systems in the region, and was the result of an iterative process to match observed hydraulic heads and spring flow. Each discharge point was given its own conduit stretch in order to distribute the spring flow as

observed in the field. Without this separation, the northernmost drain cell accounted for a large majority of the flow.

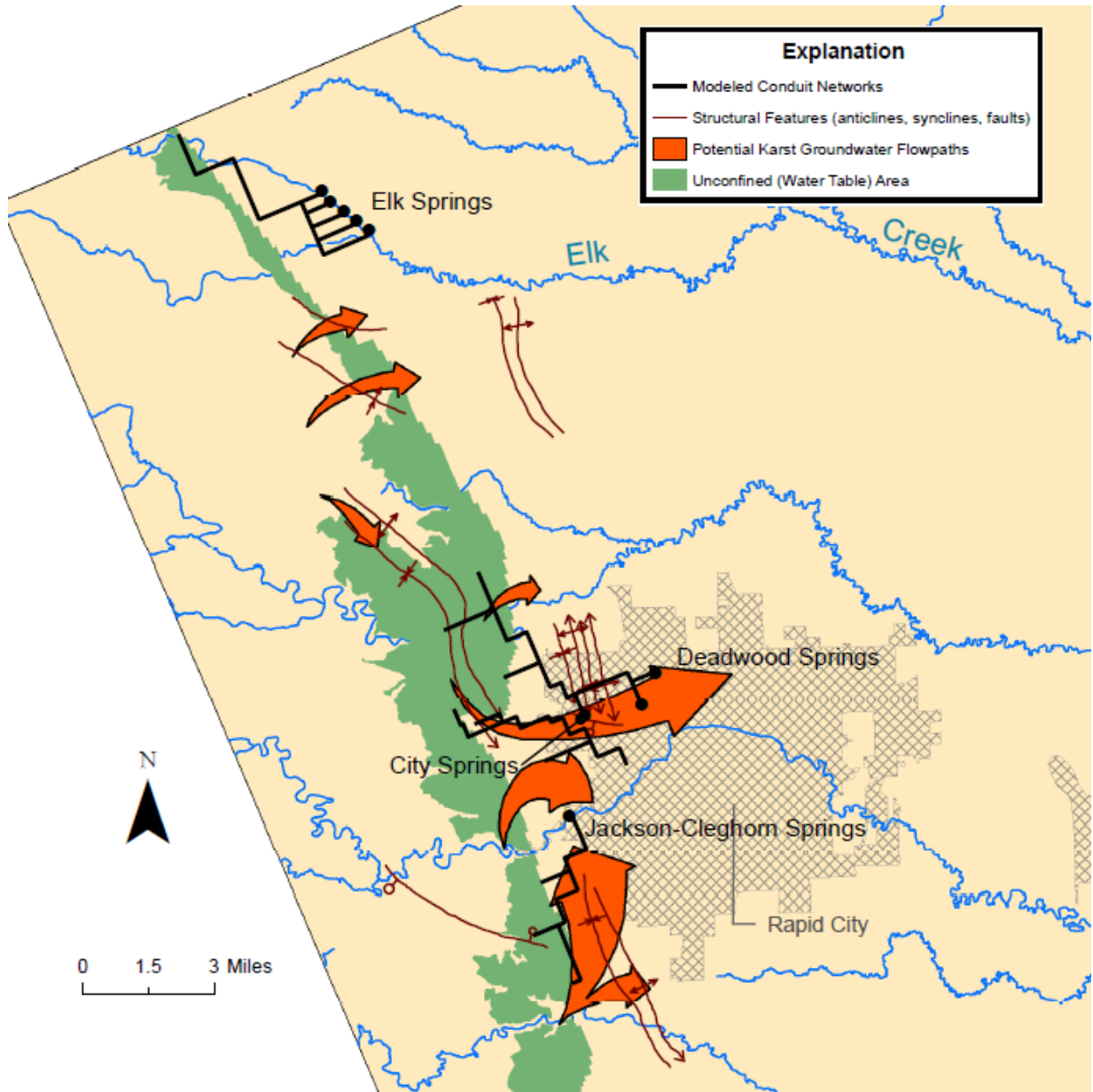


Figure 5.2 Conduit Locations

5.1.3 Conduit Parameters

Each of the six aforementioned conduit networks has multiple parameters assigned to each node within the network in a static MODFLOW-CFP input file. Within each network, those parameters were kept constant outside of two exceptions. Several parameters were kept constant throughout all the networks, primarily because of limited model sensitivity to the parameter values. CFP input parameters kept constant through the model include conduit water temperature, roughness, tortuosity, and upper and lower Reynolds numbers. Direct conduit recharge was also kept constant at zero throughout the model because no conduit was within a cell receiving direct recharge; cells receiving recharge were all within the unconfined zone of the aquifer where conduits were not modeled. A temperature of 25 degrees centigrade was kept constant throughout the model, which is the default setting of CFP and if altered does not significantly affect the model. A conduit roughness value of 0.001 ft was used throughout the model, which represents relatively smooth, longstanding karst features [Reimann and Hill, 2009]. Tortuosity was set to 1 throughout the model, which represents a straight pipe across a single finite-difference cell, and the upper and lower Reynolds numbers were set to 20 and 10 which are the CFP defaults.

The two conduit parameters that were varied within each conduit network included the node elevation and conduit wall hydraulic conductivity. Node elevation was necessary to input for each conduit cell, and was simplified to ten feet below that cell's top elevation (recall that the most significant karstification is found near the top of the Madison formation). Conduit wall conductivity is a very influential parameter in the model, and was kept consistent within each network except at the network's discharge point. At that node, to drive flow through the system, the assigned conductivity value was increased. This increase was often just one order of magnitude, but was used as a fitting parameter in matching spring discharge and often had to be raised from that point (Table 5.1).

A conduit network's diameter is another influential parameter that affects the magnitude of conduit flow and conduit-matrix exchange. Of all springs in the study area, Jackson-Cleghorn Spring has the largest measured discharge. As a result, the conduit terminating at this spring was assigned the largest fixed conduit diameter of five feet. City, Deadwood, and Elk Springs all have discharges in a similar range, and have diameters that range from 0.85 to 0.75 feet reflecting that. The non-spring conduits each have a larger diameter (1.5 and 2 ft) than the smaller scale springs in order to properly act as high conductivity pathways to feed other portions of the aquifer system.

Conduit wall hydraulic conductivity is a very sensitive parameter within each conduit network, and greatly affects the distribution of water flowing through the system. This parameter controls the exchange rate of water between the conduit and the matrix cell, and it is intended to represent the degree of connectivity of the conduit network in the form of skin effects (lesser connectivity) and microkarst features (greater connectivity). As a rule of thumb, conduit wall conductivity was initially kept near the range of the surrounding matrix conductivity of $2.65\text{E-}04$ ft/s. This value was iteratively altered as the final fitting parameter for each network, ranging between $3.00\text{E-}04$ ft/s and $1.00\text{E-}06$ ft/s. In general, the longer the conduit network, the lower the connectivity value was set. This could be explained by longer networks being more mature and having developed larger skin effects and having worn away older microkarst features. The Elk Springs conduit network had the lowest conduit wall conductivity of the spring networks because it was the only spring network to be in a lower conductivity area ($1.57\text{E-}05$ and $6.28\text{E-}05$ ft/s matrix horizontal conductivities).

An additional parameter that was adjusted to promote flow through the network toward the intended discharge location is the discharge node conduit wall conductivity. In raising this value, the connectivity of the system is improved at the sink point, which is essential for springs and helpful for the non-spring networks as well. This elevated hydraulic conductivity at the end

of a conduit network effectively represents increased permeability of the network where the water is being discharged. For most of the networks, this value was only an order of magnitude greater than the standard conduit wall conductivity. For the high discharge flow rate system of Jackson-Cleghorn Springs, this value was fitted much higher than the rest of the network at 1.0 ft/s. This would represent a much wider, more open connection to the discharge spring than the other networks.

Finally, each spring group had one or multiple corresponding drain cells that served as the outflow boundary condition. These modeled drains needed to be modified in order to limit the impact of the surrounding matrix cells on the simulated spring discharge. Each conductance was lowered from its EPM value, as seen below in Table 5.1, with the exception of Jackson-Cleghorn, which required a large value to match the observed target discharge rate of 21.6 ft³/s.

Table 5.1 Conduit Parameter Values

Conduit Networks	Network Diameter (ft)	Conduit Wall Conductivity (ft/s)	Discharge Node Conductivity (ft/s)	Drain Conductance (ft ² /s)
Jackson-Cleghorn Springs	5.00	5.00E-05	1.00E+00	13
City Springs	0.80	3.00E-04	3.00E-03	0.1
Deadwood Springs	0.75	2.00E-04	5.00E-03	0.03
Elk Springs	0.85	5.00E-06	5.00E-05	0.01
North Network	1.50	1.00E-06	1.00E-05	NA
South Network	2.0	1.00E-06	1.00E-03	NA

5.2 Steady State Model

A steady-state model of the Minnelusa and Madison aquifers was generated with conduits in order to serve as the initial condition (initial hydraulic heads). The resulting solution was similar to the prior EPM numerical model [Putnam and Long, 2009], with moderate differences primarily being found in the new unified karst conductivity zone (Figure 5.3). This

model was utilized in order to set the initial heads used at the start of the transient model. Outside of this function, it was not used in the study's model calibration.

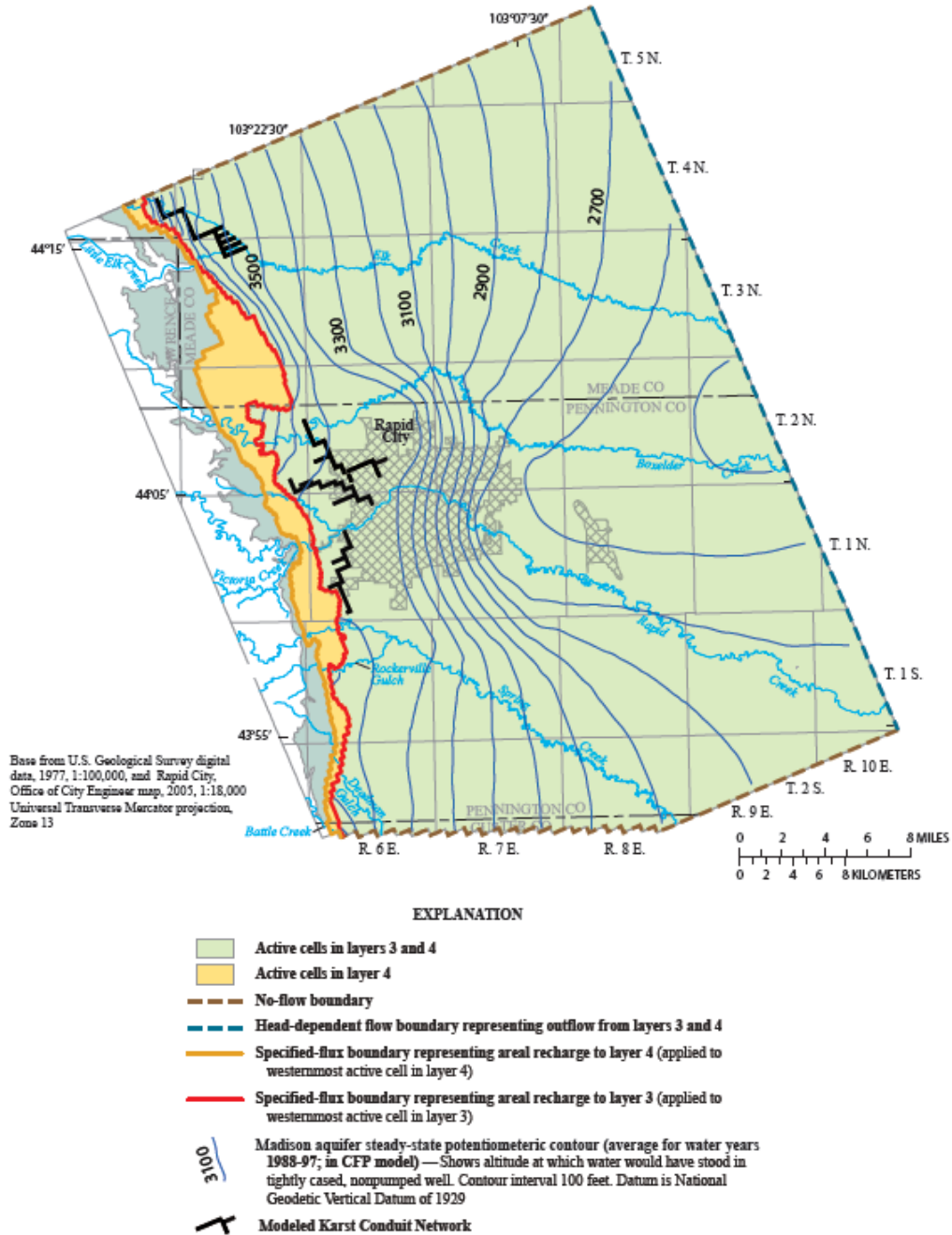


Figure 5.3 Steady State Potentiometric Surface for Model Layer 3 (modified from Putnam and Long, 2009)

5.3 Transient Model Target Data Comparisons

The target data used to evaluate the effectiveness of the new CFP model was limited to seven target wells in the Madison aquifer, and four spring discharge estimates originating from the Madison. The EPM model calibration conducted by Putnam and Long (2009) utilized several more target wells and two additional spring flow estimate locations. These observed data locations are either within the Minnelusa aquifer and therefore not used for evaluating alterations to the Madison, or were far enough away from modified zones that their value as target objectives was marginalized.

5.3.1 Comparison to Measured Hydraulic Heads at Observation Wells

Between the two sources of target data used for model calibration, average observation well hydraulic head was the more accurate (and therefore reliable) data set. Though the time frame of data collection varied, all wells showed a similar response to variations in aquifer recharge during the 10-year period. Of the seven target wells used to evaluate model calibration, six displayed large to moderate improvement over the prior EPM model in matching observed water level averages (Figure 5.6).

South of the horizontal flow barrier that divides the new karst conductivity zone there are four target wells that were influenced by two large conduit networks (Figure 5.5). The Jackson-Cleghorn karst conduit network heavily influences the entire karst zone region due to its large discharge rate. Its greatest impact is on target wells 50 and 47 due to their proximity to the spring and its down-gradient flow path zone of influence. Well 50 is located half a mile east of the drain cell representing the spring in the model, and was significantly impacted with each alteration to the network. The CFP run has raised its overall water level to better match the observed data, with the dry-period simulated heads fitting well, but wet-period heads still being

up to 10 feet lower than the 6-month average observed values. The improved fit comes from more water being brought into the system from the southern portions of the model via the conduit network, and some of that additional groundwater not leaving the system via the drainage node and migrating east. The continuing issue of the modeled data not being as responsive to the differences in recharge as the observed data is an issue ultimately caused by the simulated unconfined zone; this zone receives much of the model recharge before that water reaches the confined zone and the conduit networks therein. In a real world scenario, the conduit networks would also be found in this unconfined zone, and changes in recharge could quickly be represented in water levels even miles away. In this model, solver limitations prevented CFP nodes from being placed in unconfined areas; instead, they were placed directly outside that unconfined boundary. This limitation combined with the objective to not alter the parameters of the EPM model other than hydraulic conductivity has preserved the EPM model's responsiveness issue within target objectives. The impact of the CFP conduits can instead be evaluated on gentle numerical improvement, as seen in Well 50. Objective Well 47 is similar to 50, but much further to the east to the point of being slightly outside of the unified conductivity zone. The lower conductivity of the unified zone has prevented water from preferentially reaching well 47 in the same volume as the EPM model, and has lowered the head values up to 15 ft closer to the objective values. A closer fit would require further restructuring of the conductivity zone than was initially labeled as the karst region, and would be outside of this test's objectives.

To the north and directly between wells 50 and 47 are observation wells 43 and 46. These wells are close to the large fault represented by a horizontal flow barrier, and are not particularly close to any spring system on their side of that barrier. The water levels in both wells fluctuate heavily with each semiannual period, which indicates a strong connectivity to a conduit system in the region. Well 43, the well that is closer to the fault system, fluctuates the most, with

up to 100-ft differences between stress periods. Well 46 is located slightly further from the fault system, and exhibits more dampened fluctuations (up to 50 ft). The model fits to each of these wells are marginally improved by the CFP model, but again those large fluctuations could not be simulated with the current unconfined zone limitations.

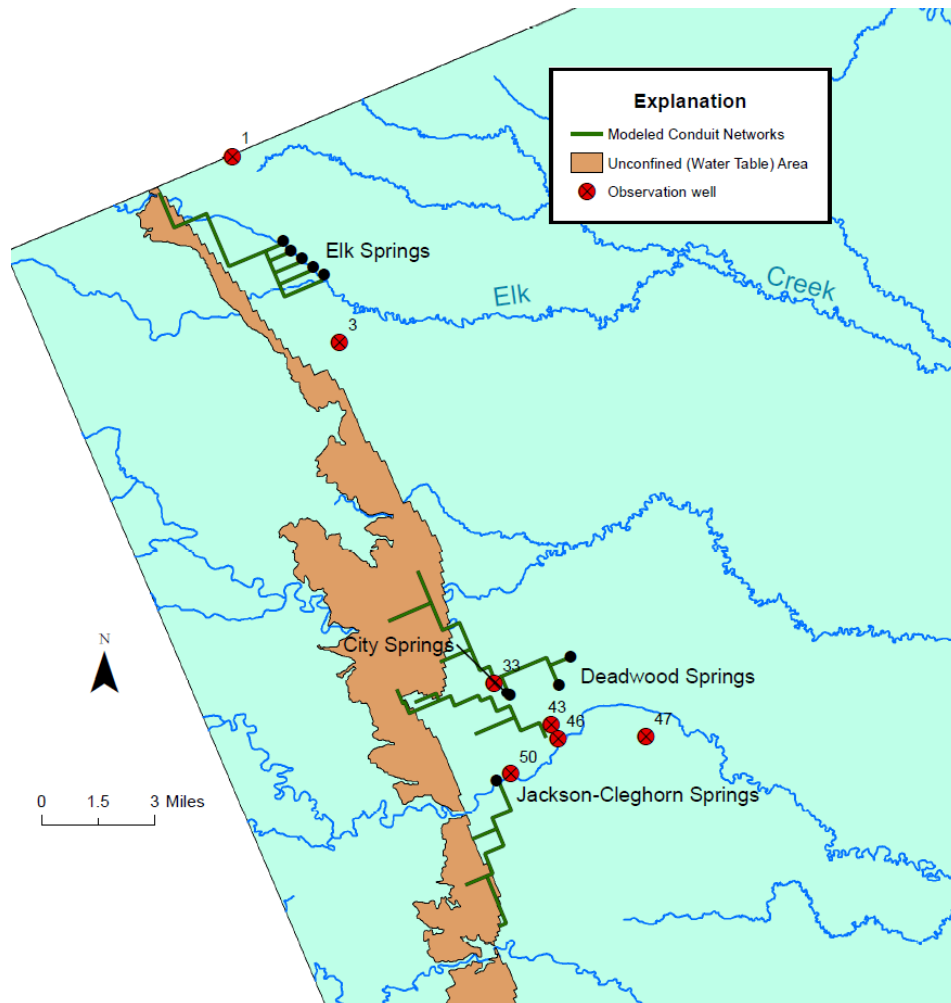


Figure 5.4 Observation Well Locations Map

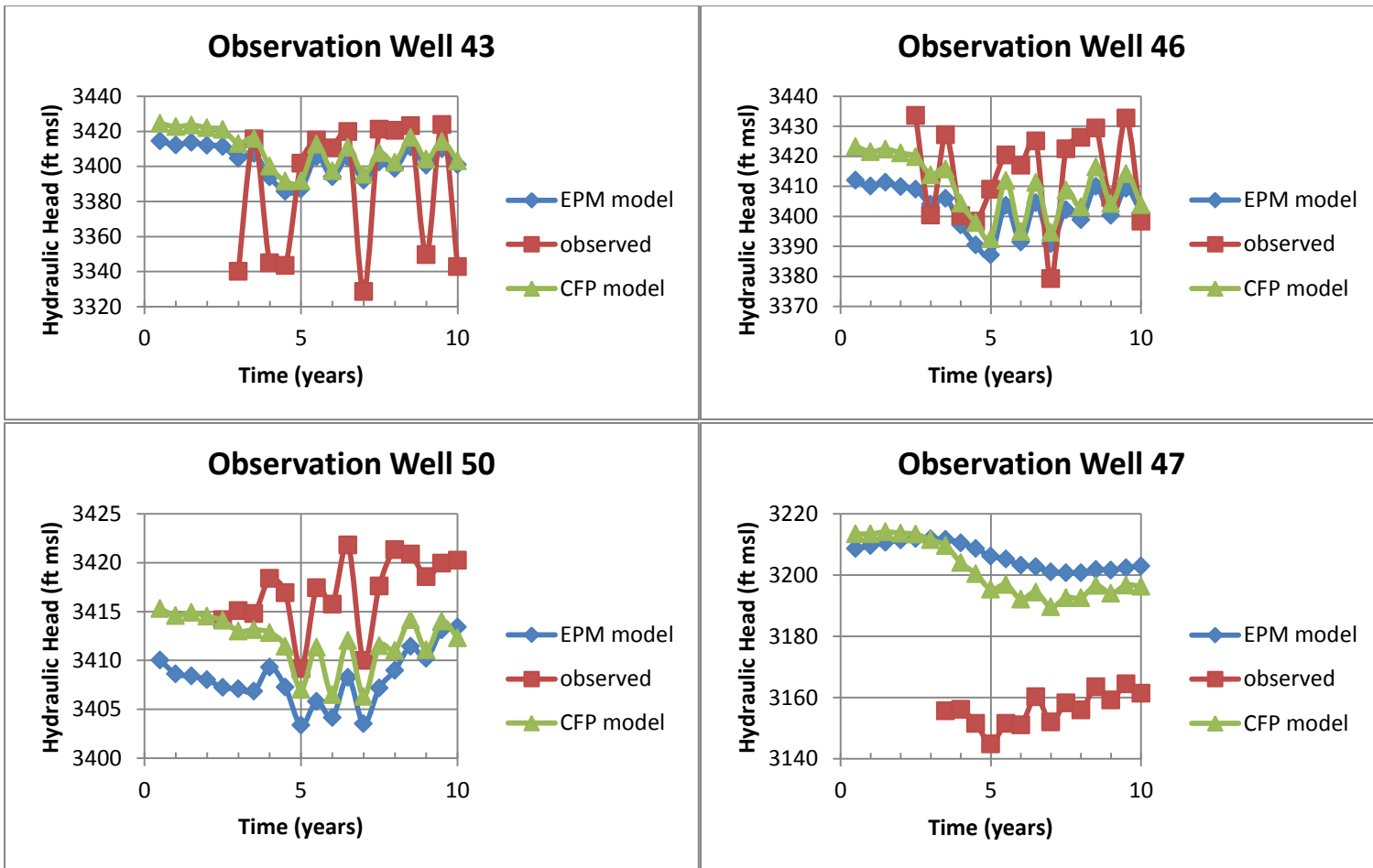


Figure 5.5 Observation Well Comparisons (part A)

North of the horizontal flow barrier there are only three Madison aquifer observation wells with transient data collected during the simulation period: target wells 1, 3 and 33. Wells 1 and 3 are directly impacted by the Elk Springs conduit network. Well 1 is located near the northern boundary of the model, north and slightly west of the Elk Springs. In the new CFP model, the simulated hydraulic head at well 1 is lowered by up to 30 ft due to the modeled conduit network that is connected to Elk Springs. The conduit network diverts flow that would have reached well 1 and brings the water levels closer to the observed data. Well 3 is the opposite - directly south of the Elk Springs, with the majority of groundwater discharged their coming from the north, less water is taken from the south, resulting in a higher hydraulic head by up to 18 ft and an improved fit to the objective data.

For the new CFP model, observation well 33 is the only target well that shows a poorer match to observations during the last half of the 10-year simulation period. During these five years, the simulated hydraulic heads were 10 to 15 ft lower than the corresponding EPM model heads. The cause can be attributed to the unique location of this target well. Near the horizontal flow barrier and between three conduit networks, the groundwater formerly running to the well was primarily taken by the City Springs and Deadwood Springs conduit systems, thereby lowering simulated heads in the neighborhood of the well. In the actual aquifer, there impact of the fault as a true no-flow barrier is possibly over-exaggerated, and water could be moving in from the east to create the observed values displayed.

In summary, the simulated hydrographs at observation wells have improved with the use of the CFP networks to varying degrees, with one exception. These measured hydraulic heads are more reliable than the spring discharge estimates that were used as the second set of objective data, and should be the primary focus for evaluating the new model with explicit conduit flow.

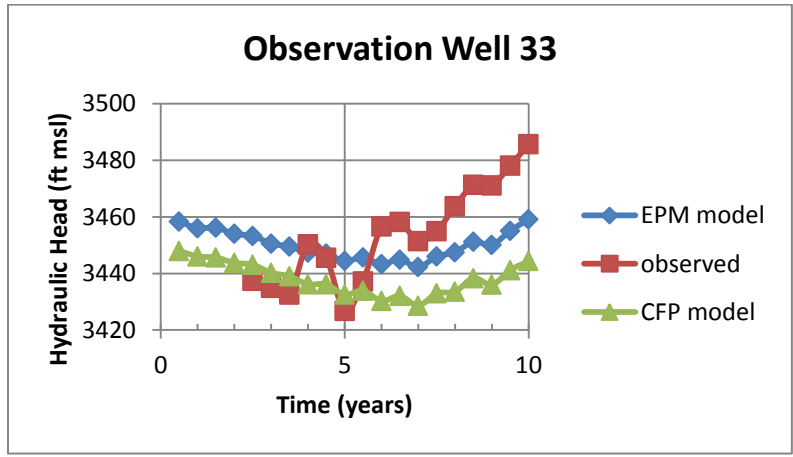
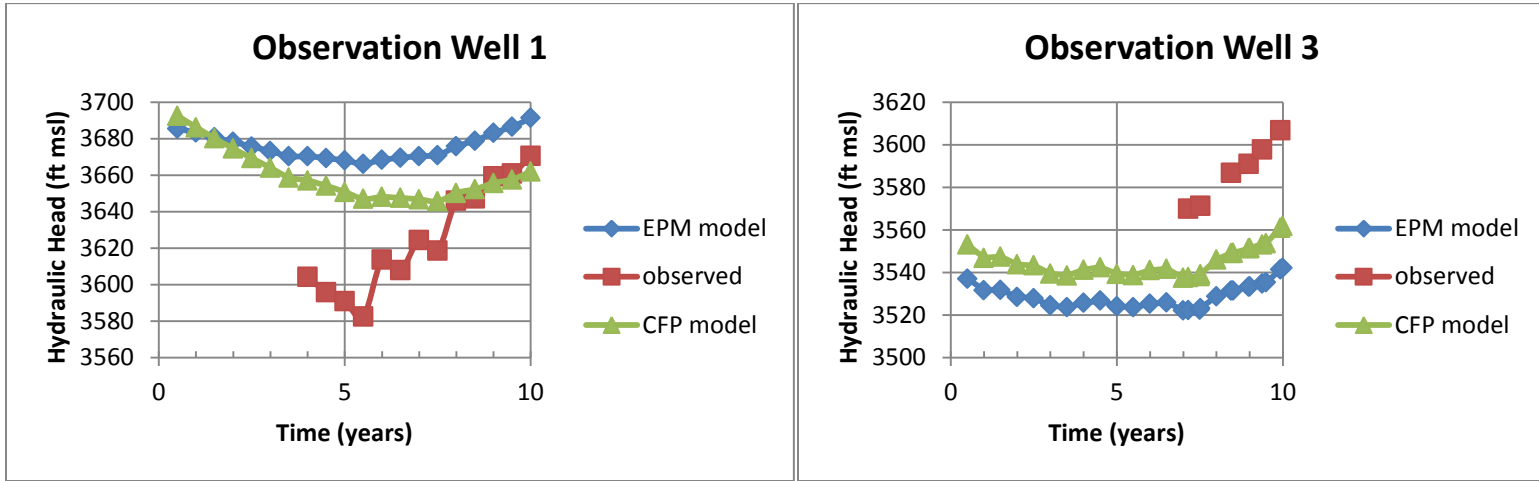


Figure 5.5 Observation Well Comparisons (part B)

5.3.2 Comparison to Estimated Spring Flow

There were four sets of estimated spring flow data in the Madison aquifer from 1987 to 1997, but two of these sets were linear averages established with volumetric balance estimates. The Jackson-Cleghorn Springs and Deadwood Springs flow estimations in Long and Putnam (2002) were set at a constant rate for the 10 year period, which in this model was kept as the target calibration objective with the understanding that the data would be used as a guideline around which an average would be found rather than a true matching objective. City Springs and Elk Springs have more dynamic estimated data, but the Elk Springs estimates present a jump in discharge magnitude unmatchable with the model objective of keeping parameters outside of hydraulic conductivity consistent with the EPM model. It is important to note that other than Jackson-Cleghorn, the other 3 spring systems found in the Madison aquifer are also modeled to be part of the Minnelusa aquifer, and the target objective data is formed from the sum the discharge from both layers. To match this, spring flow rate data below has had the simulated discharge of layer 1, which does not include CFP conduits, added to the total for each stress period. The discharge from layer 1 is typically much lower than layer 3, and is not significantly different from the layer 1 discharge in the EPM model due to the minimal influence changes in layer 3 have had on layer 1 due to the confining layer 2. The Minnelusa's contribution to the total spring flow has not been linked to karst features, and will not be featured in further discussion.

Jackson-Cleghorn Springs is the primary spring discharge point in the model, and is responsible for roughly 70% of all spring discharge in layer 3. The CFP model discharge is higher and more responsive in comparison to the EPM model, and averages out very close to the average estimated objective data at 21.59 ft³/s (Figure 5.7). The large fluctuations seen in the CFP model can reach above 3 ft³/s between stress periods, and serve as an example of the ideal positive impact of CFP providing increased recharge responsiveness. The increasingly

high flow rates in the final stress periods are a direct result of this responsiveness, and would decrease just as quickly during a more dry stress period.

Deadwood Springs has a static spring flow rate estimate objective of 2.8 ft³/s. The CFP model run improves on matching that average over the 10 year model run. During the dry period, the CFP run generates a higher flow rate level than the objective rate, and during the wet period it generates a lower flow rate. This appears contrary to what one would expect, but can be attributed to the model drawing from storage early in the life of the model due to the dry period, and the delay of the wet period's increased recharge due to the isolation of the area caused by the flow barrier to the south and the unconfined anticline to the east. Only a year after when the wet period begins does the recharge begin to increase the flow rate, which ultimately moves back toward the objective average. This is not a product of the CFP system, but rather the isolation of the area in the initial EPM model. This is reflected in the close match of discharge rates between the two systems.

City Springs has a dynamic flow rate estimate relative to the 20 stress periods, moving in response to the increase in recharge levels and growing substantially in the wet periods of the model. The CFP model and the EPM modeled rates are similar, with the conduit package averaging out higher early similar to the Deadwood system, then nearly matching in the wet period. Both of these discrepancies can be explained due to the regions isolation from recharge. As was presented previously, the actual effectiveness of the fault in completely stopping flow is probably much lower than what is modeled here.

Elk Springs also has a dynamic estimate for its discharge springflow rate, however, it is quite unique in the model and difficult to model. Essentially, for all stress periods until just after the start of the wet period the springs discharge is near zero, followed by an explosive boost in flow rate to the point where it eventually rivals Jackson-Cleghorn in discharge. As was seen in

the EPM model, even with conduits this dramatic a shift in discharge could not be modeled properly. MODFLOW-CFP does not allow for stress period dependent conduit input parameters, and without altering additional parameters the difference in area recharge is not dramatic enough to produce these levels of results. The CFP modeled discharge for Elk Springs ended up being very close to the EPM modeled results, though slightly lower overall. The actual cause of this could be something like the re-opening of filled karst conduits, or some other newly heightened connectivity level between the aquifer and the springs.

Surprisingly, the overall ebbs and flows of the spring discharge rates are not very different from what is seen from the EPM model. This can be attributed to two things: the recharge distributions being identical between the two models, and the objective levels being the same for each, resulting in similar flow rates. The greatest difference between the CFP modeled discharge and the EPM discharge is found at the most important spring, Jackson-Cleghorn. City Springs and Deadwood Springs are both isolated from much of the regional recharge and have much lower discharge rates than the other spring system. The matrix conductivity values surrounding Elk Springs were not lowered because they were already lower than the level set for the unified conductivity zone, which kept flow rates similar between the two models. The idealized impacts of using the CFP system are seen in the Jackson-Cleghorn conduit network: sharper responsiveness to alternating recharge levels and high potential flow yields. In fact, if the flat line estimates are disregarded, the large flow rate increases seen in the wet period in both City and Elk Springs are reflected well in the CFP modeled Jackson-Cleghorn system.

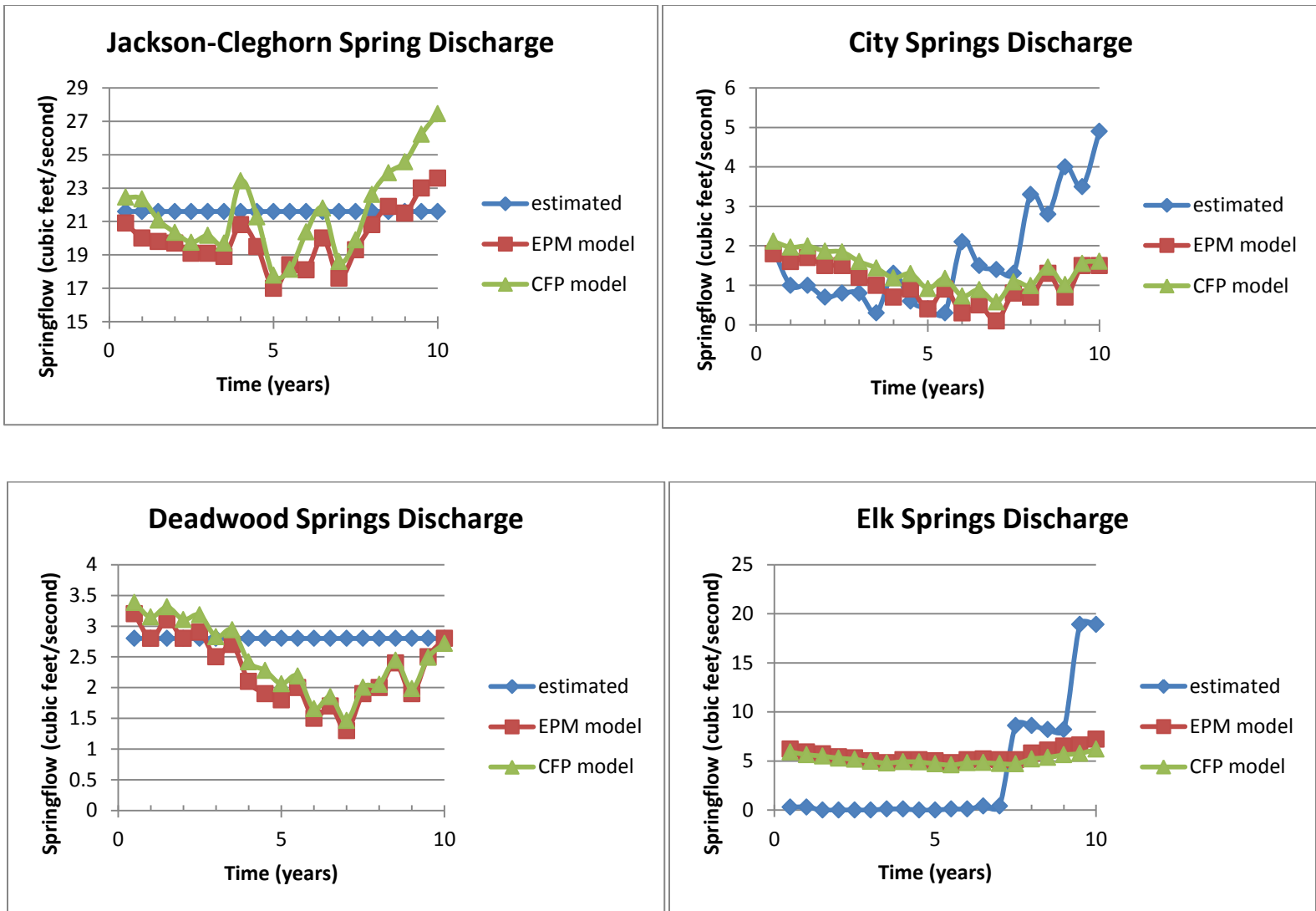


Figure 5.6 Model Comparisons to Estimated Spring Flow

5.4 Analysis of the Simulated Conduit-Matrix Exchange

A key element of the coupled continuum pipe-flow modeling framework is the exchange interactions between the conduits and matrix, and how that exchange influences the model as a whole. MODFLOW-CFP generates two interacting flow systems – a darcian flow system and a pipe flow system – and regulates the exchange between the two at each cell node by finding the hydraulic head difference between the matrix and the pipe and dampening it with an exchange coefficient. The behavior of the simulated exchange rate along distinct conduit networks provides a glimpse into how groundwater might indeed be transported throughout large karst networks.

5.4.1 Conduit-Matrix Exchange Profiles

Each conduit network has its own distinct exchange profile that changes with each stress period's shifting recharge fluxes. In this section results will be presented for two extreme cases. One is an entirely gaining, high discharge system represented by the Jackson-Cleghorn conduit network. The second is a relatively lower flow rate, non-spring feeding system that has distinct gaining and losing stretches represented by the SDET conduit network. Each behaves in different yet similar manners, and provides insight into how the modeled flow system operates and perhaps how a real karst network might operate in different situations.

The Jackson-Cleghorn Springs modeled conduit network is an extremely high flow rate system, and takes in a large amount of water from the surrounding matrix rock. As seen in figure 5.8, the majority of groundwater moving into the conduit occurs early near its starting point by Spring Creek. From there, the rate of exchange decreases and then levels off over the distance of the network. Abrupt changes in the simulated influx represent bends in the conduit network. With recharge moving from west to east through the aquifer, bends to the east gather

more groundwater by pulling contributions from the north that the network could not receive prior. With each increase in flow rate, afterward there is typically a dip that corresponds to that distance running eastward parallel to the recharge driven regional gradient. The entire track of the Jackson-Cleghorn conduit network is gaining groundwater from the matrix until its discharge point at the springs, which puts out the entire sum of the collected conduit water each stress period. Figure 5.8 provides the simulated exchange profile for two different stress periods: stress period 2 representing the dry period, and stress period 12 representing the start of the wet period. The initial influx of matrix groundwater brought into the conduit system in the wet period is nearly double the rate of the dry period, but this difference is minimized as the conduit moves north and the hydraulic head values in the conduit network reach higher levels. The peaks tend to be higher in the wet period, but near the downgradient end there is an eastern moving portion where the dry period contributes greater matrix groundwater than the wet period. This is the result of two different forces at work. One, the groundwater being contributed to in the dry period is coming out of storage, and is not available later in the model run after 5 additional dry years lowered the available storage groundwater there (at this point in the network, matrix heads are lower in stress period 12 by up to 1.5 feet). Secondly, the hydraulic head of the conduit network is higher than in stress period 2 (by up to 0.27 feet), enough to be near level with the matrix head in those cells, and due to this not bring in any matrix groundwater. Both explanations contribute to the rate difference, and demonstrate the dynamic exchange properties of the CFP network systems.

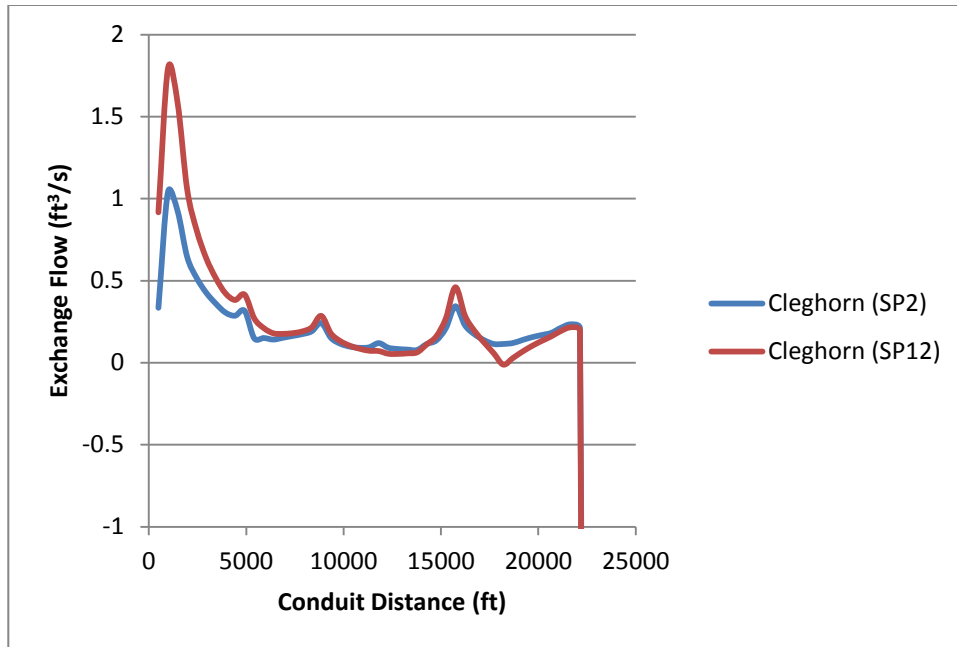


Figure 5.7 Simulated conduit-matrix exchange flow along Jackson-Cleghorn conduit network. SP2 = stress period #2 (second half of 1987 water year); SP12 = stress period #12 (second half of 1993 water year).

The SDET system is quite different from the Jackson-Cleghorn conduit network system, especially with regards to conduit-matrix exchange. Overall, the average absolute value conduit-matrix exchange for the network is less than a tenth of that simulated for the Jackson-Cleghorn network. The SDET network represents a fully submerged buried karst system that formerly possessed a discharge point, but through tectonics or other events is no longer connected with the surface. The SDET system does not end in a drain cell, and because of this the pull of water through the system is only driven by hydraulic head differences between the up-gradient and down-gradient sections of the network. This makes for a lower flow through the network, and therefore there is a gradual shift in the exchange profile from gaining to losing. Similar to the Jackson-Cleghorn graph, the exchange flow spikes at bends and declines along tracks parallel to the matrix flow gradient. The last 12,000 ft covered by this network is losing (i.e., the

hydraulic gradient is from conduit to matrix). This losing stream effect increases the matrix hydraulic head values in the vicinity of the conduit.

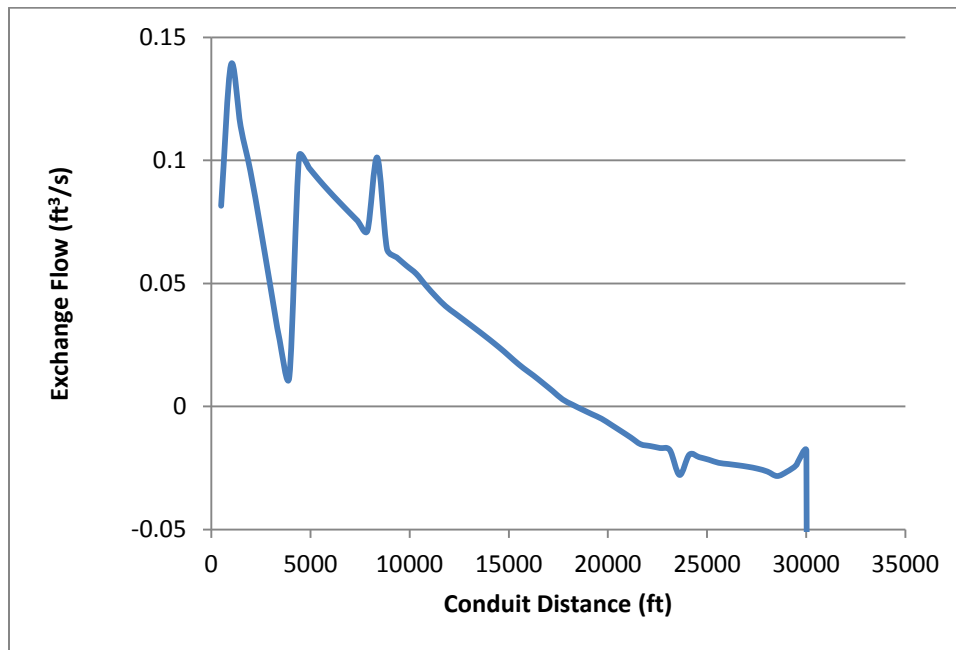


Figure 5.8 Simulated conduit-matrix exchange flow along South Network Conduit Network. Negative exchange flow indicates a losing portion of the network. Results are shown for stress period # 2.

5.4.2 Temporal Variability in Simulated Conduit-Matrix Exchange

Each of the modeled conduit networks has a different impact on the hydraulic heads in the matrix, depending on the conduit/matrix properties and recharge circumstances. The influence of conduits is best illustrated along the Jackson-Cleghorn conduit network (Figure 5.10). Two stress periods reflecting the dry and wet time frames of the modeling period were selected as evidence of this influence.

During the dry period (Figure 5.10a), the network acts as a regional sink, drawing water even from thousands of feet west of the network. The low amount of water moving into the area

leads to a lower hydraulic head in the conduit, which then creates a pull of matrix water similar to an extraction well. The pull of the conduit network generates a relatively shallow gradient along the extent of the conduit network, with a potential stagnation point to the east. On the western side of the conduit network, the steep hydraulic gradient toward the network produces a gaining conduit as seen in the exchange profiles (Figure 5.8). The regional gradient steepens significantly at the low K zone in the east in both stress periods.

The wet period hydraulic heads are quite different (Figure 5.10b). There is enough water in the system for the network not to act as a regional sink to the east. Instead, it shapes the contour profile of the region acting as a gaining stream, and reduces the regional gradient east of the network. The head contours are higher near the recharge boundary to the west, but are lower in this stress period to the east primarily due to the presence of a large municipal pumping well that was pumping at the time. The lower levels are also attributable to the amount of water available in storage having been reduced significantly over the dry period. Stress period 12 represents the early part of the wet period, and much of that water in storage has not been replaced yet.

Jackson-Cleghorn Conduit Network Contours

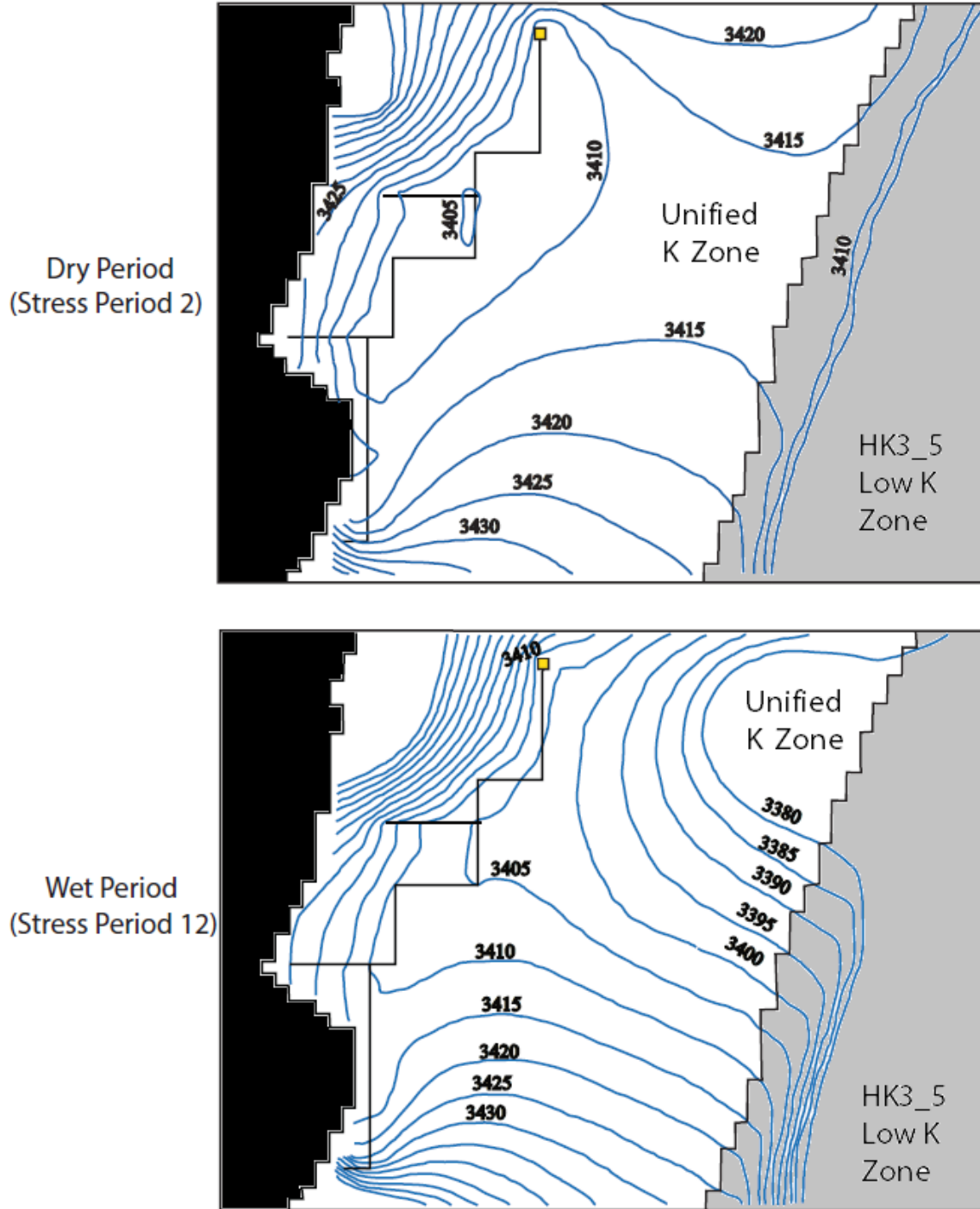


Figure 5.9 Simulated hydraulic heads in the vicinity of Jackson-Cleghorn conduit. (a) Dry period (stress period #2). (b) Wet period (stress period #12).

CHAPTER 6 – CONCLUSIONS

6.1 Study Summary

The first objective of this thesis was to integrate conduit flow into a large scale finite-difference model while maintaining numerical accuracy and model performance. Six distinct conduit networks were generated and iteratively fit into the Madison aquifer model within a framework of estimated karst pathways derived from environmental and dye tracer studies. In the new model, these networks act as the dominant groundwater flow feature within the karstified region of the aquifer. This successful application shows that the coupled continuum pipe-flow framework, and specifically its implementation in MODFLOW-CFP, may be useful for other regional scale assessments of karst aquifer dynamics.

Simplifying the horizontal conductivity zones of an EPM model previously designed to account for karst features was the second goal of this study. With these zones unified into a single matrix conductivity value, the conduit flow process networks become the primary drivers for heterogeneous flow rates within the aquifer. This brings the flow patterns within the aquifer closer to realistic conditions and simplifies the surrounding Darcian flow system inputs. Though the branching geometry of karst networks is rarely well defined, the use of a large modeled conduit network calibrated to prior flow and head data can be used to simulate the flow dynamics of a more complex actual karst system at regional scales.

Locating the networks and identifying reasonable conduit parameters would not be possible without large amounts of observed hydrology data over enough time to gather an accurate representation of the system. Replacing EPM model conductivity zones with karst conduit features resulted in a closer match to the observed transient data. This highlights the limitations of a purely Darcian flow system (EPM approach) for karst groundwater flow modeling. In this study, the modeled fit to the transient observation well data was clearly

improved by replacing the three distinct hydraulic conductivity zones with pipe flow through conduit networks in a single conductivity zone. The simulated spring discharge was similar to what had been generated previously with the EPM model, and in general was not improved with regards to the observed data. This could be the result of identical recharge patterns in each model, as well as the inherent limitations of the estimated springflow data used as observations.

The final objective of this study was to identify problematic areas in using the MODFLOW-CFP program at the regional scale, and provide suggestions as to improvements that can be made to this relatively new modeling technique. One issue that arose during the iterative installation process was the conduits interaction with the unconfined sections of the Madison aquifer. Conduit nodes in these sections were either shut down when the water table was too low, or experienced errors in the exchange process when not. A suggested improvement could involve allowing for interaction in an area to be completely disabled will still receiving direct conduit recharge. A drain type feature contained within the conduit network in addition to the constant head ability would also improve the functionality of the spring boundaries. This would eliminate the possibility of flow back into the conduit system while keeping the exit flow from needing to re-enter a matrix cell.

6.2 Proposed Future Work

Karst aquifer modeling with explicit conduit flow is still a relatively new field of study, and the MODFLOW-CFP program in particular has the possibility of being used in many transient simulation cases where the Darcian flow assumption is inadequate. There are still many avenues of research to be pursued, and with each study there is an opportunity to improve the efficiency and accuracy of this modeling technique.

One interesting and important research topic would be to further define the constraints on the conduit wall hydraulic conductance parameter in MODFLOW-CFP. It has already been shown how dependent the conduit flow and conduit-matrix exchange is on this value [Reimann and Hill, 2009], but testing and comparative analysis could be explored in order to constrain this parameter based upon the geology and hydrology of a particular aquifer system. As it stands, this conductance term primarily functions as a fitting parameter.

Another research topic that would explore the upper limits of a regional scale CFP model's functionality would be to examine its large scale use on system with much tighter time step data. The addition of conduit pipe flow to a system is best exploited in simulating specific high recharge events and the aquifer's response to those events. Data collected on a well-defined karst network at the daily or even hourly time scale could explore the limits of the CFP methodology within regional models.

The trial-and-error based iterative methods used in this study are workable, but are relatively inefficient and could be impractical for some applications. Future work should be pursued to couple MODFLOW-CFP with an inverse modeling parameter optimization system. This approach could be used to identify best-fitting conduit locations or parameters from observed data inputs. Inverse modeling with CFP may involve long computing times, since coupled numerical solutions are required for both flow domains, but would allow for parameter refinement at a level and consistency that is currently unrealistic with trial-and-error based iterative means.

Finally, and perhaps most importantly, future work should be pursued to couple the MODFLOW-CFP flow model with a solute transport model. The addition of turbulent pipe flow to an advection-dispersion-diffusion transport model would allow for more accurate contaminant transport predictions in karst aquifers. As it stands, contaminant travel times are often under

predicted, and the advised response time for municipal bodies that depend on carbonate rock aquifers for human consumption could be improved, making the general public safer.

REFERENCES

Bauer, S., Liedl, R., and Sauter, M., 2003. Modeling of karst aquifer genesis: Influence of exchange flow. *Water Resources Research*, v. 39, no. 10, p 1,285.

Bowles, C.G., and Braddock, W.A., 1963. Solution breccias of the Minnelusa Formation in the Black Hills, South Dakota and Wyoming. *Geological Survey Research 1963 - short papers in geology and hydrology, Articles 60–121. U.S. Geological Survey Professional Paper 475–C, art. 83, p. C91–C95.*

Cattermole, J.M., 1969. Geologic map of the Rapid City west quadrangle, Pennington County, South Dakota. U.S. Geological Survey Geologic Quadrangle Map GQ - 828, scale 1:24,000.

Covington, M.D., Doctor, D.H., King, J.N., Wicks, C.M., 2011. Research in karst: A model for future directions in hydrologic science? *AGU Hydrology Section, July 2011, p 18-22.*

Darnault, C. J. G., 2008. *Karst Aquifers; Hydrogeology and Exploitation NATO Science For Peace And Security Series C; Environmental Security. Netherlands: Springer : Dordrecht, Netherlands, p 203-226.*

Doherty, J., 2002. *PEST—Model independent parameter estimation, version 6. Queensland, Australia: Watermark Numerical Computing.*

Downey, J.S., 1986. *Geohydrology of bedrock aquifers in the northern Great Plains in parts of Montana, North Dakota, South Dakota, and Wyoming: U.S. Geological Survey Professional Paper 1402-E, p. 87.*

Ford, D., and Williams, P., 2007. *Karst Hydrogeology and Geomorphology. Chichester, UK. John Wiley and Sons Publishing.*

Gallegos, J.J., 2011. Modeling Groundwater Flow in Karst Aquifers: An Evaluation of MODFLOW-CFP at the Laboratory and Sub-Regional Scales. Electronic Theses, Treatises and Dissertations. Paper 4377. <http://diginole.lib.fsu.edu/etd/4377>.

Greene, E.A., 1993. Hydraulic properties of the Madison aquifer system in the western Rapid City area, South Dakota: U.S. Geological Survey Water-Resources Investigations Report 93-4008, p. 56 .

Greene, E.A., 1999. Characterizing recharge to wells in carbonate aquifers using environmental and artificially recharged tracers, in Morganwalp, D.W., and Buxton, H.T.. Proceedings of the Technical Meeting, Charleston, S.C., March 8-12, 1999, Toxic Substances Hydrology Program: U.S. Geological Survey Water-Resources Investigations Report 99-4018-C, p. 803-808.

Green, R.T., Painter, S.L., Sun, A, Worthington, S.R.H., 2006. Groundwater Contamination in Karst Terranes. WATER, AIR, & SOIL POLLUTION: FOCUS, Volume 6, Numbers 1-2 (2006), p. 157-170.

Harbaugh, A.W., 2005. MODFLOW-2005, the U.S. Geological Survey modular groundwater model—The Ground-Water Flow Process. U.S. Geological Survey Techniques and Methods 6-A16.

Hill, M., Stewart, M., and Martin, A., 2010. Evaluation of the MODFLOW-2005 Conduit Flow Process. *Ground Water*, 48(4), 549-559.

Liedl, R, Sauter, M, Huckinghaus, D, Clemens, T, Teutsch, G, 2003. Simulation of the development of karst aquifers using a coupled continuum pipe flow model. *Water Resources Research*, volume 39, issue 3, article 1057.

Long, A.J., Putnam, L.D., 2002. Flow-system analysis of the Madison and Minnelusa aquifers in the Rapid City area, South Dakota—conceptual model. U.S. Geological Survey Water-Resources Investigations Report 02–4185.

Long, A.J., Sawyer, J.F., Putnam, L.D., 2008. Environmental tracers as indicators of karst conduits in groundwater in South Dakota, USA. *Hydrogeology Journal*, v. 16, no. 2, p. 263–280.

Naus, C.A., Driscoll, D.G., Carter, J.M., 2001. Geochemistry of the Madison and Minnelusa aquifers in the Black Hills area, South Dakota. U.S. Geological Survey Water-Resources Investigations Report 01-4129, p. 118.

Putnam, L.D., and Long, A.J., 2007, Analysis of ground-waterflow in the Madison aquifer using fluorescent dyes injected in Spring Creek and Rapid Creek near Rapid City, South Dakota, 2003–04: U.S. Geological Survey Scientific Investigations Report 2007–5137, p. 27.

Putnam, L.D., Long, A.J., 2009. Numerical Groundwater-Flow Model of the Minnelusa and Madison Hydrogeologic Units in the Rapid City Area, South Dakota. U.S. Geological Survey Water-Resources Investigations Report 09–5205.

Quinn, J. J., Tomasko, D., Kuiper J. A., 2006. Modeling Complex Flow In A Karst Aquifer. *Sedimentary Geology* 184.3-4, p. 343-351.

Reimann, T., Hill, M. E., 2009. MODFLOW-CFP; A New Conduit Flow Process For MODFLOW-2005. *Ground Water* 47.3, p. 321-325.

Saller, S.P., and M.J. Ronayne (2011), A comparison of single-continuum and dual-conductivity karst aquifer models during recharge events, Abstract H23F-1339. Presented at 2011 Fall Meeting, AGU, San Francisco, Calif., 5-9 Dec.

Scanlon, B.R., Mace, R.E., Barrett, M.E., Smith, B., 2003. Can we simulate regional groundwater flow in a karst system using equivalent porous media models? Case study, Barton

Springs Edwards aquifer, United States of America. *Journal of Hydrology*, volume 276, p. 137–158.

Shoemaker, W.B., Kuniatsky, E.L., Birk, S., Bauer, S., Swain, E.D., 2008. Documentation of a Conduit Flow Process (CFP) for MODFLOW-2005. U.S. Geological Survey Techniques and Methods, Book 6, Chapter A24.

Strobel M.L., Jarrell, G.J., Sawyer, J.F., Schleicher, J.R., Fahrenbach, M.D., 1999. Distribution of hydrogeologic units in the Black Hills area, South Dakota. U.S. Geological Survey Hydrologic Investigations Atlas HA-743, 3 sheets, scale 1:100,000.

Teutsch, G., 1993. An extended double-porosity concept as a practical modelling approach for a karstified terrain. *Hydrogeology Processes in Karst Terranes*, Proc. of the Antalya Symp. And Field Seminar, Oct. 1990, International Association Hydrology Science Publication No. 207, p. 281–292.

Worthington, S.R.H., 2009. Diagnostic hydrogeologic characteristics of a karst aquifer (Kentucky, USA). *Hydrogeology Journal*. Volume 17, p. 1665–1678.

Worthington S.R.H. & Ford D.C., 2009. Self-Organized Permeability in Carbonate Aquifers. *Ground Water*, Volume 47, p. 326-336.